Diagrammatic approaches to the inelastic propagator

B. Feuerbacher* and L. S. Cederbaum

Theoretische Chemie, Physikalisch-Chemisches Institut, Universität Heidelberg

Im Neuenheimer Feld 229, D-69120 Heidelberg, Germany

Abstract

Two different diagrammatic construction schemes for obtaining the propagator for inelastic electronic scattering are presented. Both are discussed for the three cases that the target molecule of interest is closed-shell itself or has a closed-shell anion or cation. The "direct approach" yields the inelastic propagator directly, but has the drawback that it requires the evaluation of a large number of diagrams already in low orders. The "Dyson approach" uses Dyson-like equations for the inelastic propagator and employs a diagrammatic construction scheme for the generalized one-particle densities only. It therefore requires a considerably lower number of diagrams. Results are given up to first order for both methods and all three cases. Alternative approaches are briefly discussed and compared with our methods.

PACS numbers: 34.80.Gs, 03.65.Nk, 31.10.+z

*Electronic address: Bjoern.Feuerbacher@pci.uni-heidelberg.de

I. INTRODUCTION

Green's functions provide a powerful tool for studying the properties of many-body systems, in elementary particle physics as well as in nuclear, atomic and molecular physics. They can be used to describe properties of bound states (see e. g. [1–5]) as well as scattering: As shown already in [6], the usual one-particle Green's function (also called the propagator) obeys a Dyson equation, where the self-energy is an optical potential [7] for *elastic* scattering. The theory for calculating the propagator for elastic scattering and with it the scattering matrix, phase shifts and resonance energies is well-developed and has been in wide use for several decades now [8–14].

In contrast, only very few attempts were made to also treat *inelastic* scattering with Green's function methods (see e. g. the pioneering work of Csanak et al.[15, 16]). Inelastic scattering processes involve excited states of molecules, and such systems are out-of-equilibrium. Keldysh has developed a diagrammatic technique for dealing with such systems forty years ago [17], but his approach deals mainly with statistical systems under the action of an external field. In contrast, we are concerned here with transitions of molecules between well-defined excited states.

In recent years, a formally exact theory for inelastic scattering of *non-electronic* projectiles from molecular targets was developed [18, 19]. This case is simpler than the scattering of electrons, since the projetile is distinguishable from the particles of the target. For the case where the projectile is indistinguishable from the target particles, the situation is much more complicated [20–22]. There also exists a method for the exact treatment of the inelastic scattering of electrons for the case that rotational and vibrational degrees of freedom of the target molecule are excited [23].

What is still missing is a systematic diagrammatic method for explicitly evaluating the inelastic propagator for transitions between electronically excited states. In contrast, diagrammatic evaluation procedures for the elastic propagator have long been known and used in the literature (e. g. the Algebraic Diagrammatic Construction scheme [1]). In this work, we address this open problem by presenting two different diagrammatic approaches for calculating the inelastic propagator.

An additional, at first sight unrelated problem is that the standard Green's function methods work only for closed-shell molecules. Promising attempts were made to extend

them also to open-shell systems [24, 25], but again a systematic diagrammatic treatment of the problem is missing. The methods we will present for calculating the inelastic propagator are also applicable to scattering off molecules which only have a closed-shell anion or cation, but are open-shell in their neutral state. Hence they can open up the opportunity to study elastic as well as inelastic propagators for open-shell molecules. We will show that the diagrammatic treatment of such molecules with our methods is even easier than the application to scattering off closed-shell molecules.

Section II first briefly reviews the various possible definitions for the inelastic propagator discussed in [21] and then illustrates a "direct" approach for obtaining these propagators. Since this approach has the drawback that the evaluation of a large number of diagrams is required even in low orders, section III describes an alternative method, employing the Dyson-like equation for the particle component of the inelastic propagator developed in [21]. A Dyson-like equation for the hole component is also presented there, and it is demonstrated for the first time how one can completely separate the two time-orderings of the propagator. Then, it is outlined how one can obtain the generalized one-particle densities occuring in the Dyson-like equations by using a diagrammatic approach. Finally, section IV summarizes our results and compares our methods with other approaches for obtaining the inelastic propagator or the generalized one-particle densities.

II. DIRECT CALCULATION OF THE INELASTIC PROPAGATOR

A. Various possible definitions for the inelastic propagator

In [21], it was shown that in order to ensure energy conservation, the inelastic propagator has to be defined by

$$\begin{aligned} iG_{pq}^{+[M,N]}(\tau) &= \theta(\tau) < M|c_p(t)c_q^\dagger(t')|N > e^{i\Phi^{+[M,N]}(t,t')} \\ iG_{pq}^{-[M,N]}(\tau) &= -\theta(-\tau) < M|c_q^\dagger(t')c_p(t)|N > e^{i\Phi^{-[M,N]}(t,t')} \end{aligned} \tag{1}$$

where

$$G_{pq}^{[M,N]}(\tau) = G_{pq}^{+[M,N]}(\tau) + G_{pq}^{-[M,N]}(\tau),$$

and the phases have to satisfy

$$\Phi^{+[M,N]}(t,t') = -(E^{[M]} - E^{[0]})t + (E^{[N]} - E^{[0]})t' + F^{+[M,N]}(\tau) \tag{2}$$

$$\Phi^{-[M,N]}(t,t') \;=\; -(E^{[M]}-E^{[0]})t' + (E^{[N]}-E^{[0]})t + F^{-[M,N]}(\tau).$$

The c_p and $c_q^\dagger$ are the usual destruction and creation operators, $E^{[0]}$ is the energy of the ground state $|0>$, and the $E^{[M]}$ are the energies of the excited states $|M>$. The $F^{\pm[M,N]}$ are arbitrary functions of the time difference $\tau = t-t'$. For faciliating the Fourier transformation of the propagator, it is convenient to choose these functions to be linear:

$$F^{\pm[M,N]}(\tau) = f^{\pm[M,N]}\tau$$

with constant factors $f^{+[M,N]}$ and $f^{-[M,N]}$.

Three different possible choices for the phases were studied in detail in [21]. Note that for all of them, $G^{[0,0]}_{pq}$ is identical to the usual text book propagator, which we may call the "elastic propagator".

1. One can choose the $f^{\pm[N,M]}$ simply to be zero. The resulting propagator is called the "natural" Green's function and will be denoted with a "n" in its superscript.

2. It was pointed out in [21] that many calculations can be simplified if the two phases are the same. Since in scattering processes, essentially only the particle component G^+ of the propagator is needed, it is sensible to keep the phase of that part the same as before and only change the phase for the hole component. The resulting propagator is called the "scattering-motivated" Green's function and will be denoted with a "s" in its superscript. The corresponding phases are:

$$\Phi^{+s[M,N]}(t,t') = \Phi^{-s[M,N]}(t,t') = -(E^{[M]}-E^{[0]})t + (E^{[N]}-E^{[0]})t', \tag{3}$$

   i. e. $f^{+[M,N]} = 0$ and $f^{-[M,N]} = -E^{[M]} - E^{[N]} + 2E^{[0]}$.

3. Finally, it turns out that if one wants to study ionization processes instead of scattering, it is convenient to change the particle component G^+ and keep the hole component of the natural Green's function. The resulting propagator is called the "ionization-motivated" Green's function and will be denoted with an "i" in its superscript. The corresponding phases are:

$$\Phi^{+i[M,N]}(t,t') = \Phi^{-i[M,N]}(t,t') = -(E^{[M]}-E^{[0]})t' + (E^{[N]}-E^{[0]})t \tag{4}$$

   i. e. $f^{-[M,N]} = 0$ and $f^{+[M,N]} = E^{[M]} + E^{[N]} - 2E^{[0]}$. In contrast to [21], we have not exchanged the order of the indices N, M here, for reasons which will soon become clear.

In the following, we will outline how one can obtain the inelastic Green's function for transitions between electronically excited states directly. We will demonstrate the method for three different types of molecules from which the electron is scattered:

1. The molecule is closed-shell itself.

2. The molecule has a closed-shell anion.

3. The molecule has a closed-shell cation.

Hence when one calculates the inelastic propagator, one has, compared to the elastic propagator, the additional advantage that this can not only be done for closed-shell molecules, but is also possible if the molecule only has a closed-shell anion or cation. Actually, it will turn out that these cases are even easier to treat than the case of a closed-shell molecule, and are very similar to each other.

The method described in this section will be referred to as the *direct approach* in the following.

B. Closed-shell molecule

The main idea of all approaches discussed here is to use higher Green's functions, which are defined with respect to the ground state of the closed-shell molecule of interest (or the corresponding ion), and hence can be computed using the standard Feynman diagram methods. The spectral representations of these higher Green's functions then establish a connection with the desired inelastic propagators.
Here we define the six-point, four-times Green's function

$$
\begin{aligned}
& iR_{pqrstu}(t_f,t,t',t_i) \qquad (5)\\
= & -<0|\hat{T}\left[c_p^\dagger(t_f)c_q(t_f)c_r(t)c_s^\dagger(t')c_t^\dagger(t_i)c_u(t_i)\right]|0> \\
& +<0|\hat{T}\left[c_p^\dagger(t_f)c_q(t_f)c_r(t)c_s^\dagger(t')\right]|0><0|c_t^\dagger(t_i)c_u(t_i)|0> \\
& +<0|\hat{T}\left[c_r(t)c_s^\dagger(t')c_t^\dagger(t_i)c_u(t_i)\right]|0><0|c_p^\dagger(t_f)c_q(t_f)|0> \\
& +<0|\hat{T}\left[c_p^\dagger(t_f)c_q(t_f)c_t^\dagger(t_i)c_u(t_i)\right]|0><0|\hat{T}\left[c_r(t)c_s^\dagger(t')\right]|0> \\
& -2<0|c_p^\dagger(t_f)c_q(t_f)|0><0|\hat{T}\left[c_r(t)c_s^\dagger(t')\right]|0><0|c_t^\dagger(t_i)c_u(t_i)|0>,
\end{aligned}
$$

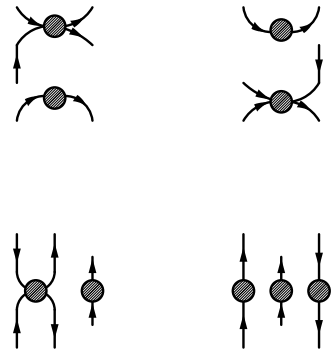

FIG. 1: Disjoint diagrams which do not contribute to the four-times Green's function for a closed-shell molecule

where the factorized terms which are subtracted or added to eliminate disjoint diagrams of the general structure shown in Fig. 1 in the diagrammatic expansion, and the overall sign is chosen to give a convenient spectral representation. The time indices "f" and "i" mean "final" and "initial", respectively. $\hat{T}$ denotes the usual time ordering operator.

The natural interpretation of this higher-order Green's function is that at the time t_i, an excitation of the molecule of interest is created, and at time t_f, another excitation is destroyed. These two excited states serve as the background on which the propagation of an electron (or a hole) is studied. We will show below in detail how far this intuitive picture of the meaning of this Green's function indeed holds true.

Note that the six-point, six-times Green's function was already discussed extensively in [26]; we concentrate here on the special case of four times and show how it can be applied to the problem at hand.

There are $4! = 24$ different time orderings possible for this Green's function. All quantities depend only on the three time differences $\tau_f = t_f - t$, $\tau = t - t'$ and $\tau_i = t' - t_i$, and hence we can write:

$$\begin{aligned} R_{pqrstu}(t_f, t, t', t_i) &= \theta(\tau_f)\theta(\tau)\theta(\tau_i) R^{(I)}_{pqrstu}(\tau_f, \tau, \tau_i) \\ &+ \theta(\tau_f)\theta(-\tau)\theta(\tau_i) R^{(II)}_{pqrstu}(\tau_f, \tau, \tau_i) \\ &+ \ldots \end{aligned}$$

For the first four time orderings, we choose:

I. $t_f > t > t' > t_i$

II. $t_f > t' > t > t_i$

III. $t_i > t > t' > t_f$

IV. $t_i > t' > t > t_f$

The remaining 20 time orderings give rise to contributions which are not of interest here.

1. *Connection to the inelastic propagator*

We treat here only the first time ordering in detail and give later the results for the second to fourth orderings briefly. We denote these four contributions to R corresponding to the above introduced time orderings by $R^{(I)}$, $R^{(II)}$, $R^{(III)}$ and $R^{(IV)}$. For $t_f > t > t' > t_i$, one obtains the simplified expression

$$\begin{aligned} & iR^{(I)}_{pqrstu}(t_f,t,t',t_i) \\ = & - <0|c_p^\dagger(t_f)c_q(t_f)(1-|0><0|)c_r(t)c_s^\dagger(t')(1-|0><0|)c_t^\dagger(t_i)c_u(t_i)|0> \\ & - <0|c_p^\dagger(t_f)c_q(t_f)(1-|0><0|)c_t^\dagger(t_i)c_u(t_i)|0><0|c_r(t)c_s^\dagger(t')|0> . \end{aligned}$$

Writing the 1 using a complete set yields:

$$\begin{aligned} iR^{(I)}_{pqrstu}(t_f,t,t',t_i) = & - \sum_{M\neq 0, N\neq 0} <0|c_p^\dagger(t_f)c_q(t_f)|M><N|c_t^\dagger(t_i)c_u(t_i)|0> \\ & \cdot \Big(<M|c_r(t)c_s^\dagger(t')|N> - \delta_{MN} <0|c_r(t)c_s^\dagger(t')|0> \Big) . \end{aligned}$$

Using the time dependence of the destruction and creation operators and introducing the *generalized one-particle densities*

$$\rho^{[N,M]}_{pq} = <N|c_p^\dagger c_q|M>, \tag{6}$$

one can rewrite $R^{(I)}$ to take on the following appearance:

$$\begin{aligned} iR^{(I)}_{pqrstu}(\tau_f,t,t',\tau_i) = & - \sum_{M\neq 0, N\neq 0} \rho^{[0,M]}_{pq}\rho^{[N,0]}_{tu} e^{-i(E^{[M]}-E^{[0]})\tau_f} e^{-i(E^{[N]}-E^{[0]})\tau_i} \\ & \cdot \Big(<M|c_r(t)c_s^\dagger(t')|N> - \delta_{MN} <0|c_r(t)c_s^\dagger(t')|0> \Big) \\ & \cdot e^{-i(E^{[M]}-E^{[0]})t} e^{+i(E^{[N]}-E^{[0]})t'} . \end{aligned}$$

With the definition of the particle component of the natural inelastic Green's function $G^{+n[N,M]}$, one readily finds the interrelation

$$\begin{aligned} R^{(I)}_{pqrstu}(\tau_f,\tau,\tau_i) \;=\; & -\sum_{M\neq 0,N\neq 0} \rho^{[0,M]}_{pq}\rho^{[N,0]}_{tu} e^{-i(E^{[M]}-E^{[0]})\tau_f} e^{-i(E^{[N]}-E^{[0]})\tau_i} \\ & \cdot \left(G^{+n[M,N]}_{rs}(\tau) - \delta_{MN} G^{+[0,0]}_{rs}(\tau) e^{-i(E^{[M]}-E^{[0]})\tau} \right). \end{aligned}$$

Fourier transforming with respect to τ_f and τ_i gives:

$$\begin{aligned} R^{(I)}_{pqrstu}(\omega_f,\omega_i,\tau) \;=\; & \sum_{M\neq 0,N\neq 0} \frac{\rho^{[0,M]}_{pq}}{\omega_f - (E^{[M]}-E^{[0]}) + i0^+} \frac{\rho^{[N,0]}_{tu}}{\omega_i - (E^{[N]}-E^{[0]}) + i0^+} \\ & \cdot \left(G^{+n[M,N]}_{rs}(\tau) - \delta_{MN} G^{+[0,0]}_{rs}(\tau) e^{-i(E^{[M]}-E^{[0]})\tau} \right). \end{aligned} \tag{7}$$

The poles of this Green's function (in both ω_f and ω_i) are seen to be given by the energy differences between the excited states and the ground state of the system, and the residues of the double poles are

$$\rho^{[0,M]}_{pq} \left(G^{+n[M,N]}_{rs}(\tau) - \delta_{MN} G^{+[0,0]}_{rs}(\tau) e^{-i(E^{[M]}-E^{[0]})\tau} \right) \rho^{[N,0]}_{tu}. \tag{8}$$

Hence one can determine the particle component of the natural inelastic Green's function from the residues of the higher elastic Green's function. In order to actually obtain the inelastic Green's function, one has to eliminate the generalized densities $\rho^{[0,M]}_{pq}$ and $\rho^{[N,0]}_{tu}$ in (8). In section II B 3, we will demonstrate how this can be done by studying the structure of the perturbatively obtained expressions and identifying the contributions of the different terms. Alternatively, one can try to obtain these generalized densities from a different source, e. g. from the residues of the polarization propagator [27, 28], and then simply divide them out.

A look at eq.(8) shows that one needs to know the elastic Green's function in order to obtain $G^{+[M,N]}_{rs}(t,t')$. It is possible to avoid this problem by defining R alternatively in the following way:

$$\begin{aligned} & iR_{pqrstu}(t_f,t,t',t_i) \\ = \; & - < 0|\hat{T}\left[c^\dagger_p(t_f)c_q(t_f)c_r(t)c^\dagger_s(t')c^\dagger_t(t_i)c_u(t_i)\right]|0> \\ & + < 0|\hat{T}\left[c^\dagger_p(t_f)c_q(t_f)c_r(t)c^\dagger_s(t')\right]|0>< 0|c^\dagger_t(t_i)c_u(t_i)|0> \\ & + < 0|\hat{T}\left[c_r(t)c^\dagger_s(t')c^\dagger_t(t_i)c_u(t_i)\right]|0>< 0|c^\dagger_p(t_f)c_q(t_f)|0> \\ & - < 0|c^\dagger_p(t_f)c_q(t_f)|0>< 0|\hat{T}\left[c_r(t)c^\dagger_s(t')\right]|0>< 0|c^\dagger_t(t_i)c_u(t_i)|0>, \end{aligned} \tag{9}$$

i. e. one subtracts less terms than in the original definition. The result for the spectral decomposition is then simply:

$$R^{(I)}_{pqrstu}(\omega_f,\omega_i,t,t') = \sum_{M,N\neq 0} \frac{\rho^{[0,M]}_{pq} G^{+n[M,N]}_{rs}(t,t')\rho^{[N,0]}_{tu}}{(\omega_f - (E^{[M]}-E^{[0]})+i0^+)(\omega_i-(E^{[N]}-E^{[0]})+i0^+)}. \qquad (10)$$

To evaluate this interrelation, it is now necessary to include the third type of disjoint diagrams shown in Fig. 1. The number of diagrams one has to consider is already quite high even without these disjoint diagrams, and experience will show which definition of R is more useful. Of course, one could simply take the expressions for the elastic Green's function from the literature.

Using the same mathematical steps to evaluate $R^{(II)}$ as used above for $R^{(I)}$, one obtains for this component:

$$\begin{aligned} iR^{(II)}_{pqrstu}(\tau_f,t,t',\tau_i) \;=\; + \sum_{M\neq 0,N\neq 0} & \rho^{[0,M]}_{pq}\rho^{[N,0]}_{tu} e^{-i(E^{[M]}-E^{[0]})\tau_f} e^{-i(E^{[N]}-E^{[0]})\tau_i} \\ & \cdot \Big(< M|c^\dagger_s(t')c_r(t)|N> - \delta_{MN} < 0|c^\dagger_s(t')c_r(t)|0> \Big) \\ & \cdot e^{-i(E^{[M]}-E^{[0]})t} e^{+i(E^{[N]}-E^{[0]})t'}. \end{aligned}$$

Here, not the natural inelastic Green's function, but rather the hole component of the scattering motivated inelastic Green's function appears. This relation gives after Fourier transformation (note that here the time variables are now subject to the constraints $\tau_f > -\tau$, $\tau_i > -\tau$):

$$\begin{aligned} R^{(II)}_{pqrstu}(\omega_f,\omega_i,\tau) \;=\; + \sum_{M\neq 0,N\neq 0} & \frac{\rho^{[0,M]}_{pq} e^{-i(\omega_f-(E^{[M]}-E^{[0]}))\tau}}{\omega_f-(E^{[M]}-E^{[0]})+i0^+} \frac{\rho^{[N,0]}_{tu} e^{-i(\omega_i-(E^{[N]}-E^{[0]}))\tau}}{\omega_i-(E^{[N]}-E^{[0]})+i0^+} \\ & \cdot \Big(G^{-s[M,N]}_{rs}(\tau) - \delta_{MN} G^{-[0,0]}_{rs}(\tau) e^{-i(E^{[M]}-E^{[0]})\tau)} \Big). \qquad (11) \end{aligned}$$

The exponential functions appearing here drop out when one calculates the residues in order to obtain $G^{-s[M,N]}_{rs}$ from $R^{(II)}_{pqrstu}(\omega_f,\omega_i,\tau)$.

For the third component, one finds:

$$\begin{aligned} iR^{(III)}_{pqrstu}(\tau_f,t,t',\tau_i) \;=\; + \sum_{M\neq 0,N\neq 0} & \rho^{[0,M]}_{tu}\rho^{[N,0]}_{pq} e^{i(E^{[N]}-E^{[0]})\tau_f} e^{i(E^{[M]}-E^{[0]})\tau_i} \\ & \cdot \Big(< M|c_r(t)c^\dagger_s(t')|N> - \delta_{MN} < 0|c_r(t)c^\dagger_s(t')|0> \Big) \\ & \cdot e^{-i(E^{[M]}-E^{[0]})t'} e^{+i(E^{[N]}-E^{[0]})t}, \end{aligned}$$

which can be rewritten using the particle component of the ionization-motivated inelastic Green's function. This yields:

$$R^{(III)}_{pqrstu}(\omega_f,\omega_i,\tau) \;=\; -\sum_{M\neq 0,N\neq 0}\frac{\rho^{[0,M]}_{tu}e^{-i(\omega_i+(E^{[M]}-E^{[0]}))\tau}}{\omega_i+(E^{[M]}-E^{[0]})-i0^+}\frac{\rho^{[N,0]}_{pq}e^{-i(\omega_f+(E^{[N]}-E^{[0]}))\tau}}{\omega_f+(E^{[N]}-E^{[0]})-i0^+}$$
$$\cdot\left(G^{+i[M,N]}_{rs}(\tau)-\delta_{MN}G^{+[0,0]}_{rs}(\tau)e^{i(E^{[M]}-E^{[0]})\tau)}\right). \qquad (12)$$

Again, the exponential functions appearing here drop out when expressing the inelastic Green's function by $R^{(III)}$.

Finally, for the fourth component one arrives at

$$iR^{(IV)}_{pqrstu}(\tau_f,t,t',\tau_i) \;=\; +\sum_{M\neq 0,N\neq 0}\rho^{[0,M]}_{tu}\rho^{[N,0]}_{pq}e^{i(E^{[N]}-E^{[0]})\tau_f}e^{i(E^{[M]}-E^{[0]})\tau_i}$$
$$\cdot\left(<M|c^\dagger_s(t')c_r(t)|N>-\delta_{MN}<0|c^\dagger_s(t')c_r(t)|0>\right)$$
$$\cdot e^{-i(E^{[M]}-E^{[0]})t'}e^{+i(E^{[N]}-E^{[0]})t},$$

for which now again the natural Green's function can be used, here its hole component (which is the same as the hole component of the ionization-motivated inelastic Green's function), yielding

$$R^{(IV)}_{pqrstu}(\omega_f,\omega_i,\tau) \;=\; -\sum_{M\neq 0,N\neq 0}\frac{\rho^{[0,M]}_{tu}}{\omega_i+(E^{[M]}-E^{[0]})-i0^+}\frac{\rho^{[N,0]}_{pq}}{\omega_f+(E^{[N]}-E^{[0]})-i0^+}$$
$$\cdot\left(G^{-n[M,N]}_{rs}(\tau)-\delta_{MN}G^{-[0,0]}_{rs}(\tau)e^{i(E^{[M]}-E^{[0]})\tau)}\right). \qquad (13)$$

In summary, the first and the fourth time ordered components of the elastic quantity R determine completely the natural inelastic Green's function. Analogously, the first and the second components provide us with the scattering-motivated inelastic Green's function, and the third and the fourth components give the ionization-motivated inelastic Green's function.

For brevity, we now introduce the following notation for residues:

$$\mathrm{Res}_{x,x_0}f(x)=\lim_{x\to x_0}(x-x_0)f(x)$$

Then one can write explicitly:

$$\rho^{[0,M]}_{pq}\left(G^{s[M,N]}_{rs}(\tau)-\delta_{MN}G^{[0,0]}_{rs}(\tau)e^{-i\tau(E^{[M]}-E^{[0]})}\right)\rho^{[N,0]}_{tu} \qquad (14)$$
$$=\;\mathrm{Res}_{\omega_f,E^{[M]}-E^{[0]}}\mathrm{Res}_{\omega_i,E^{[N]}-E^{[0]}}\left(R^{(I)}_{pqrstu}(\omega_f,\omega_i,\tau)+R^{(II)}_{pqrstu}(\omega_f,\omega_i,\tau)\right)$$

$$\rho_{tu}^{[0,M]}\left(G_{rs}^{i[M,N]}(\tau)-\delta_{MN}G_{rs}^{[0,0]}(\tau)e^{-i\tau(E^{[M]}-E^{[0]})}\right)\rho_{pq}^{[N,0]} \tag{15}$$
$$= -\mathrm{Res}_{\omega_f,-E^{[N]}+E^{[0]}}\mathrm{Res}_{\omega_i,-E^{[M]}+E^{[0]}}\left(R_{pqrstu}^{(III)}(\omega_f,\omega_i,\tau)+R_{pqrstu}^{(IV)}(\omega_f,\omega_i,\tau)\right).$$

In other words, one can obtain both components of the scattering-motivated inelastic Green's functions together from a single expression, and the same holds true also for the ionization-motivated inelastic Green's function. In contrast, one has to combine different formulas if one wants to obtain the two components of the natural inelastic Green's function:

$$\rho_{pq}^{[0,M]}\left(G_{rs}^{+n[M,N]}(\tau)-\delta_{MN}G_{rs}^{+[0,0]}(\tau)e^{-i\tau(E^{[M]}-E^{[0]})}\right)\rho_{tu}^{[N,0]} \tag{16}$$
$$= \mathrm{Res}_{\omega_f,E^{[M]}-E^{[0]}}\mathrm{Res}_{\omega_i,E^{[N]}-E^{[0]}}R_{pqrstu}^{(I)}(\omega_f,\omega_i,\tau)$$

$$\rho_{tu}^{[0,M]}\left(G_{rs}^{-n[M,N]}(\tau)-\delta_{MN}G_{rs}^{-[0,0]}(\tau)e^{-i\tau(E^{[M]}-E^{[0]})}\right)\rho_{pq}^{[N,0]} \tag{17}$$
$$= -\mathrm{Res}_{\omega_f,-E^{[N]}+E^{[0]}}\mathrm{Res}_{\omega_i,-E^{[M]}+E^{[0]}}R_{pqrstu}^{(IV)}(\omega_f',\omega_i',\tau).$$

Finally, let us remark than one can use the time differences $\tau_f'=t_f-t'$ and $\tau_i'=t-t_i$ as an alternative choice to τ_f and τ_i used above. This leads to similar interrelations between the inelastic propagator we are looking for and the elastic quantity R:

$$\rho_{pq}^{[0,M]}\left(G_{rs}^{i[M,N]}(\tau)-\delta_{MN}G_{rs}^{[0,0]}(\tau)e^{-i\tau(E^{[M]}-E^{[0]})}\right)\rho_{tu}^{[N,0]} \tag{18}$$
$$= \mathrm{Res}_{\omega_f',E^{[M]}-E^{[0]}}\mathrm{Res}_{\omega_i',E^{[N]}-E^{[0]}}\left(R_{pqrstu}^{(I)}(\omega_f',\omega_i',\tau)+R_{pqrstu}^{(II)}(\omega_f',\omega_i',\tau)\right)$$

$$\rho_{tu}^{[0,M]}\left(G_{rs}^{s[M,N]}(\tau)-\delta_{MN}G_{rs}^{[0,0]}(\tau)e^{-i\tau(E^{[M]}-E^{[0]})}\right)\rho_{pq}^{[N,0]} \tag{19}$$
$$= -\mathrm{Res}_{\omega_f',-E^{[N]}+E^{[0]}}\mathrm{Res}_{\omega_i',-E^{[M]}+E^{[0]}}\left(R_{pqrstu}^{(III)}(\omega_f',\omega_i',\tau)+R_{pqrstu}^{(IV)}(\omega_f',\omega_i',\tau)\right)$$

for the scattering- and ionization-motivated inelastic Green's function, and

$$\rho_{tu}^{[0,M]}\left(G_{rs}^{+n[M,N]}(\tau)-\delta_{MN}G_{rs}^{+[0,0]}(\tau)e^{-i\tau(E^{[M]}-E^{[0]})}\right)\rho_{pq}^{[N,0]} \tag{20}$$
$$= -\mathrm{Res}_{\omega_f',-E^{[N]}+E^{[0]}}\mathrm{Res}_{\omega_i',-E^{[M]}+E^{[0]}}R_{pqrstu}^{(III)}(\omega_f',\omega_i',\tau)$$

$$\rho_{pq}^{[0,M]}\left(G_{rs}^{-n[M,N]}(\tau)-\delta_{MN}G_{rs}^{-[0,0]}(\tau)e^{-i\tau(E^{[M]}-E^{[0]})}\right)\rho_{tu}^{[N,0]} \tag{21}$$
$$= \mathrm{Res}_{\omega_f',E^{[M]}-E^{[0]}}\mathrm{Res}_{\omega_i',E^{[N]}-E^{[0]}}R_{pqrstu}^{(II)}(\omega_f',\omega_i',\tau)$$

for the natural inelastic Green's function.

It is also worth pointing out that by making use of the fact that the residues of the polarization propagator Π^{+}_{pqtu} [27, 28] are given by

$$\rho^{[0,M]}_{pq}\rho^{[M,0]}_{tu},$$

one can write down the following explicit expression for the inelastic propagator in the special case $N = M$:

$$\begin{aligned} G^{+n[M,M]}_{rs}(\tau) \;=\; & \frac{\mathrm{Res}_{\omega_f,E^{[M]}-E^{[0]}}\mathrm{Res}_{\omega_i,E^{[M]}-E^{[0]}}R^{(I)}_{pqrstu}(\omega_f,\omega_i,\tau)}{\mathrm{Res}_{\omega,E^{[M]}-E^{[0]}}\Pi^{+}_{pqtu}(\omega)} \\ & + G^{+[0,0]}_{rs}(\tau)e^{-i(E^{[M]}-E^{[0]})\tau}. \end{aligned} \tag{22}$$

Analagous relations hold for the other components and other possible definitions of the inelastic propagator.

2. Diagrammatic representation

In order to evaluate the Green's functions, it is convenient to use the concept of Feynman diagrams and rules. They can be found in standard textbooks on the quantum mechanics of many-particle systems, e.g. [28]. We present them here for the special case of our higher elastic Green's function R and employ them in the next subsection to obtain diagrams for the inelastic propagators. Thereby we use the Hamiltonian

$$H = \sum_p \epsilon_p c^{\dagger}_p c_p + \sum_{pq} W_{pq} c^{\dagger}_p c_q - \frac{1}{2}\sum_{abcd} V_{abcd} c^{\dagger}_a c^{\dagger}_b c_c c_d \tag{23}$$

and the Hartree-Fock one-particle interaction

$$W_{pq} = -\sum_n V_{pn[qn]} n_n, \tag{24}$$

with the one-particle (orbital) energies ϵ_p and the occupation numbers n_p. The quantities

$$V_{abcd} = < \phi_a(1)\phi_b(2)|V(1,2)|\phi_c(1)\phi_d(2) >$$

denote the matrix elements of the two-particle interaction with respect to the one-particle states $|\phi_a >$, and the abbreviation

$$V_{ab[cd]} = V_{abcd} - V_{abdc} = V_{abcd} - V_{bacd} = V_{[ab]cd}$$

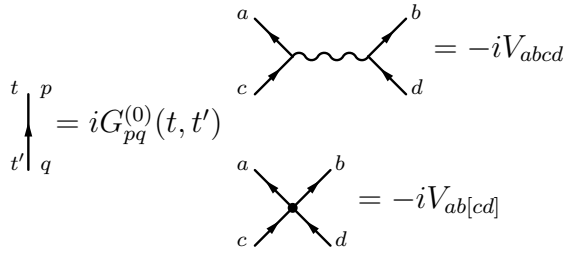

FIG. 2: Feynman rules for the elements of the diagrams

is used for the antisymmetrized matrix elements.

The rules for the Feynman diagrams in order n are:

(F1) Draw all topologically distinct connected diagrams with n interaction (wavy) lines and $2n+3$ directed free Green's function (solid) lines, where one solid line starts at time t', one ends at time t, and at times t_i and t_f, both one line starts and one ends.

(F2) Skip all disjoint graphs, i.e., graphs of the structure shown in Fig. 1. Such terms are exactly canceled by the additional terms in the definition of R.

(F3) Label the graphs with one-particle indices and time arguments according to Fig. 2. This figure also defines the graphical symbols. The free Green's function appearing in the rule for the fermion lines is given by:

$$iG^{(0)}_{pq}(t,t') = \delta_{pq} e^{-i\epsilon_p(t-t')} \left(\bar{n}_p \theta(t-t') - n_p \theta(t'-t)\right) \tag{25}$$

with $\bar{n}_p = 1 - n_p$. Sum over all internal indices and integrate over all internal times.

(F4) Multiply by a sign factor $(-1)^L$, where L is the number of closed (fermion) loops and by an additional factor i stemming from the definition of R. Each Green's function line contributes a factor $+i$, each vertex a factor $-i$. Hence when all i-factors for a nth order diagram are collected, one obtains the overall factor

$$i(-i)^n(i)^{2n+3} = i^n.$$

There is also an additional sign factor arising from the way in which the external times t_f, t, t' and t_i are connected to each other by fermion lines. The sign is $+1$ for the connections

- t_f to t_f, t_i to t_i, t to t'
- t_f to t, t_i to t', t_f to t_i

- t_f to t', t_i to t, t_f to t_i

and -1 for the remaining possible connections

- t_f to t_i, t_f to t_i, t to t'
- t_f to t, t_f to t', t_i to t_i
- t_i to t, t_i to t', t_f to t_f

Employing the Abrikosov notation, i.e., replacing the wavy interaction lines by interaction points representing the antisymmetrized matrix elements $V_{ab[cd]}$, reduces the number of diagrams considerably, although the overall sign is not uniquely determined in this notation.

(F5) The correct sign of the graph follows from the comparison with the sign of one Feynman graph which is contained in the Abrikosov graph.

(F6) As an additional rule for Abrikosov graphs, one has to multiply each graph by 2^{-P}, where P is the number of permutations of two G^0 lines leaving the graph topologically unchanged.

The evaluation of an nth order Feynman diagram $X(t_f, t, t', t_i)$ requires the performance of n time integrations over the internal time indices $t_1, \ldots, t_n$. The result of these integrations and of the additional Fourier transformations

$$X(\omega_f, \omega_i, \omega) = \int_{-\infty}^{\infty} e^{i\omega_f \tau_f} e^{i\omega_i \tau_i} e^{i\omega\tau} X(\tau_f, \tau_t, \tau) d\tau_f d\tau_i d\tau$$

can be read directly off the so-called Goldstone diagrams. The sum of the contributions from all diagrams gives then $R_{pqrstu}(\omega_f, \omega_i, \omega)$. From this, one can obtain $\mathbf{G}(\omega)$ and then $\mathbf{G}(\tau)$ by a reverse Fourier transformation. It would be desirable to obtain $R_{pqrstu}(\omega_f, \omega_i, \tau)$ and thereby $\mathbf{G}(\tau)$ directly from such a diagrammatic expansion, but unfortunately this does not seem to be easily possible.

The rules to draw and evaluate the Goldstone diagrams are as follows:

(G1) For a given nth order Feynman diagram, draw all $(n+4)!$ time-ordered diagrams which result from permuting the ordering of the times $t_f, t, t', t_i, t_1, \ldots, t_n$. We further introduce three auxiliary lines connecting the pairs of external times (t_f,t), (t,t'), and (t',t_i), going from the first to the second time in all three cases.

(G2) For the Goldstone diagrams, the direction of the lines has a meaning: Upwards- and downwards-directed lines represent particles (unoccupied one-particle states) and holes

(occupied one-particle states), respectively. Label all such lines with one-particle indices respecting this distinction (n or $\bar{n}$).

(G3) Each cut (a horizontal line) between two successive vertices (including the external vertices) introduces a denominator of the type

$$\sigma_f\omega_f + \sigma_i\omega_i + \sigma\omega + \epsilon_k + \epsilon_l + \ldots - \epsilon_i - \epsilon_j - \ldots + i0^+.$$

Here each cut line gives a contribution: hole-lines $k, l, \ldots$ contribute the one-particle energies $\epsilon_k, \epsilon_l, \ldots$; particle lines $i, j, \ldots$ contribute the negative energies $-\epsilon_i, -\epsilon_j, \ldots$. The energy variables ω_f, ω_i and ω are introduced if the corresponding auxiliary line is cut, and have positive ($\sigma_f = +1$, $\sigma_i = +1$, or $\sigma = +1$, respectively) or negative signs ($\sigma_f = -1$, $\sigma_i = -1$, or $\sigma = -1$, respectively), according to the downward or upward direction of the corresponding auxiliary line. If none of the auxiliary lines is cut, then $\sigma_f = \sigma_i = \sigma = 0$, and a constant denominator results, in which the imaginary infinitesimal $i0^+$ can be omitted.

(G4) Each hole line introduces the factor (-1). Thus, multiply by a sign factor $(-1)^{L+M}$, where L is the number of closed loops and M is the number of hole lines. Since each vertex gives a factor $-i$ and each of the $n+3$ cuts (between the $n+4$ vertices) gives a factor $+i$, one obtains together with the factor i from the definition of R the overall factor $i(-i)^n(i)^{n+3} = +1$.

Additionally one has to multiply with a sign factor depending on the way in which the external times are connected (see rule F4).

One may also employ the Abrikosov notation for the Goldstone diagrams; the corresponding rules (G5) and (G6) are analogous to (F5) and (F6).

The $(n+4)!$ Goldstone diagrams can be divided into 24 classes of diagrams according to the 24 possible time orderings of t_f, t, t' and t_i for the external vertices. The diagrams contribute then only to the respective parts of R. The number of Feynman diagrams in order n (Abrikosov notation) is:

- $n = 0$: 2
- $n = 1$: 6
- $n = 2$: 36

For a given time ordering of the external vertices in order n, one has to consider $(n+4)!/4!$ (=1, 5, 30, ...) different Goldstone diagrams for every Feynman diagram. Hence the number

FIG. 3: Goldstone diagrams for the first component $R^{(I)}$ of the four-times Green's function for a closed-shell molecule in zeroth order

of Goldstone diagrams for a given time ordering of the external vertices is in order n (if one uses the Abrikosov notation):

- $n = 0$: 2 (Fig. 3)
- $n = 1$: 30 (Fig. 4)
- $n = 2$: 1080

For the second order, the 36 Feynman diagrams are shown in Fig. 5. In all Feynman diagrams, the dotted lines are inserted to denote the four times t_f, t, t', and t_i. The auxiliary lines mentioned in rule (G1) are not shown explicitly.

3. Evaluation of the diagrams up to first order

In leading order, the relation between the first component of the four-times Green's function and the particle component of the inelastic propagator is simply

$$\begin{aligned} R^{(I)(0)}_{pqrstu}(\omega_f, \omega_i, \omega) \;=\; & \frac{\rho^{[0,q\bar{p}](0)}_{pq}}{\omega_f - (E^{[q\bar{p}]} - E^{[0]})^{(0)} + i0^+} \frac{\rho^{[t\bar{u},0]^{(0)}}_{tu}}{\omega_i - (E^{[t\bar{u}]} - E^{[0]})^{(0)} + i0^+} \\ & \cdot \left(G^{+n[q\bar{p},t\bar{u}](0)}_{rs}(\omega) - \delta_{qt}\delta_{pu} G^{+[0,0](0)}_{rs} \left(\omega - (E^{[t\bar{u}]} - E^{[0]})^{(0)} \right) \right), \end{aligned} \tag{26}$$

where we wrote $q\bar{p}$ for a $1p1h$ excitation (particle state q and hole state p). On the other hand, the evaluation of the two diagrams of Fig. 3 yields

$$\begin{aligned} R^{(I)(0)}_{pqrstu}(\omega_f, \omega_i, \omega) \;=\; & \frac{n_p \bar{n}_q \bar{n}_t n_u}{(\omega_f - \epsilon_q + \epsilon_p + i0^+)(\omega_i - \epsilon_t + \epsilon_u + i0^+)} \\ & \cdot \left[\frac{\delta_{pr}\delta_{qt}\delta_{su}}{\omega - \epsilon_t + i0^+} - \frac{\delta_{qs}\delta_{pu}\delta_{rt}}{\omega - \epsilon_s - \epsilon_r + \epsilon_u + i0^+} \right] \end{aligned} \tag{27}$$

Using additionally that

$$G^{+[0,0]}_{rs}(\omega) = \frac{\delta_{rs}\bar{n}_s}{\omega - \epsilon_s + i0^+},$$

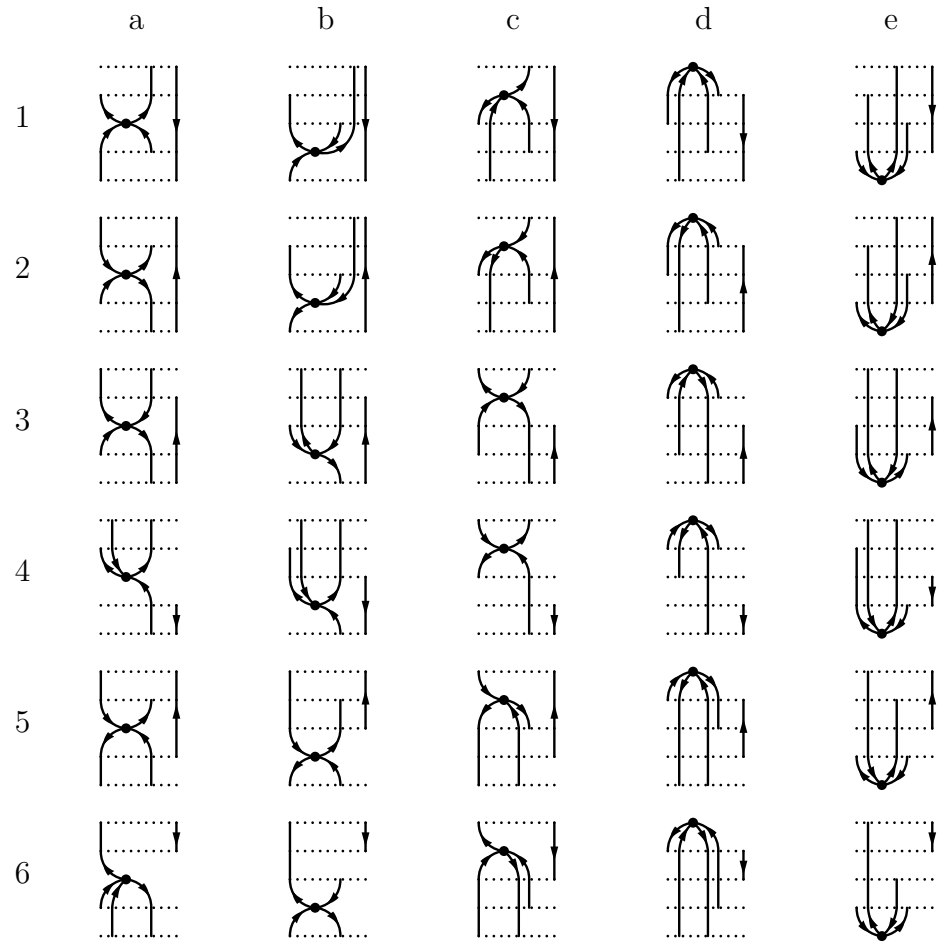

FIG. 4: Goldstone diagrams for the first component $R^{(I)}$ of the four-times Green's function for a closed-shell molecule in first order

we readily find

$$\rho_{pq}^{[0,q\bar{p}](0)} = n_p \bar{n}_q \tag{28}$$

$$\rho_{tu}^{[t\bar{u},0](0)} = \bar{n}_t n_u \tag{29}$$

$$\left(E^{[q\bar{p}]} - E^{[0]}\right)^{(0)} = \epsilon_q - \epsilon_p \tag{30}$$

$$G_{rs}^{+n[q\bar{p},t\bar{u}](0)}(\omega) = \frac{\delta_{pr}\delta_{qt}\delta_{su}}{\omega - \epsilon_t + i0^+} - \frac{\delta_{qs}\delta_{pu}\delta_{rt}}{\omega - \epsilon_s - \epsilon_r + \epsilon_u + i0^+} - \frac{\delta_{qt}\delta_{pu}\delta_{rs}\bar{n}_s}{\omega + \epsilon_p - \epsilon_q - \epsilon_r + i0^+}, \tag{31}$$

in agreement with the results which one can easily obtain by a straightforward perturbative evaluation.

In contrast to the zeroth order, where only one state $|p\bar{q}>$ contributes to the sums, *all*

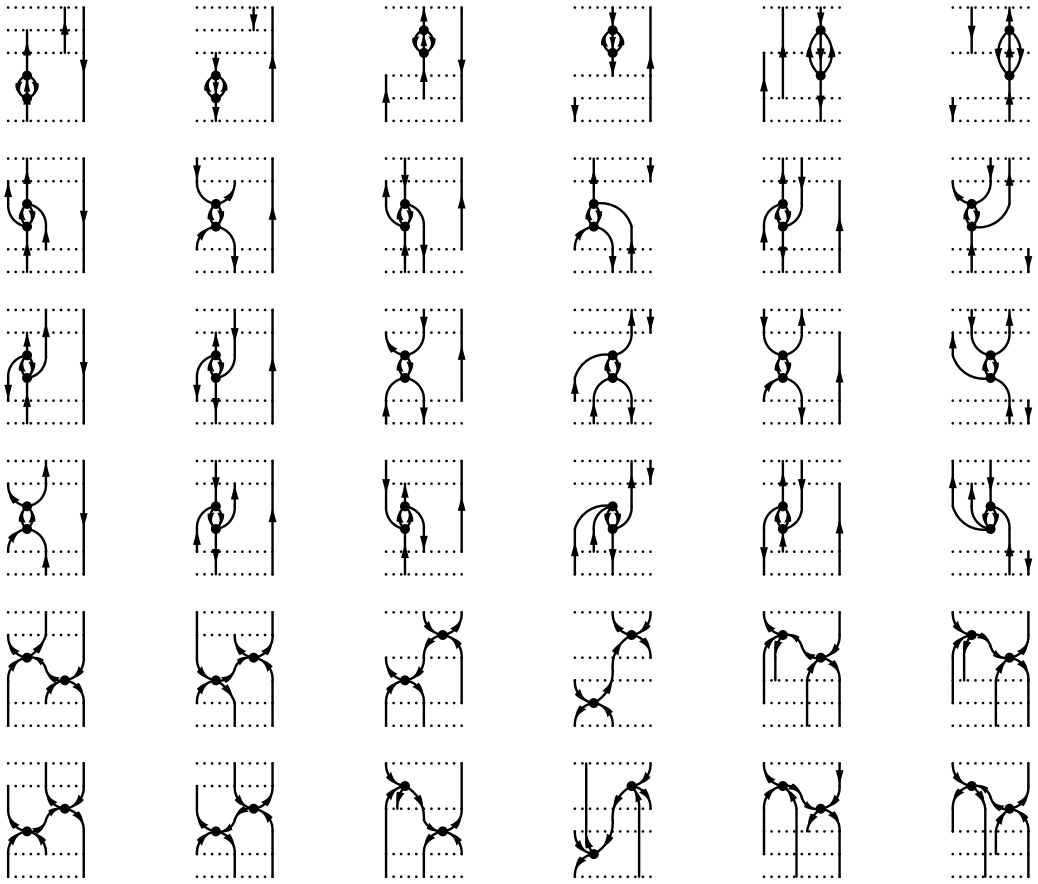

FIG. 5: Feynman diagrams for the four-times Green's function for a closed-shell molecule in second order

$1p-1h$ excitations, and additionally also $2p-2h$ excitations contribute in firsrt order. For analyzing all the different contributions arising from the 30 diagrams shown in Fig. 4, it is convenient to introduce vectors $\mathbf{T}_{tu}$ containing the generalized densities $\rho_{tu}^{[N,0]}$ for *fixed* t,u and matrices $\mathbf{G}_{rs}(\omega)$ for the propagators

$$G_{rs}^{+n[M,N]}(\omega) - \delta_{MN} G_{rs}^{+[0,0]}\left(\omega - (E^{M]} - E^{[0]})\right)$$

for *fixed* r,s (the vector and matrix indices run over the excited states). Further, we introduce the *diagonal* matrices $\mathbf{E}$ and $\mathbf{V}$, where the diagonal elements of $\mathbf{E}$ are the leading order contributions to the energy differences $E^{[M]} - E^{[0]}$, and $\mathbf{V}$ contains the higher orders. Then one can write:

$$R_{pqrstu}^{(I)}(\omega_f, \omega_i, \omega) = \mathbf{T}_{qp}^{\dagger} \frac{1}{\omega_f - \mathbf{E} - \mathbf{V}} \mathbf{G}_{rs}(\omega) \frac{1}{\omega_i - \mathbf{E} - \mathbf{V}} \mathbf{T}_{tu}. \tag{32}$$

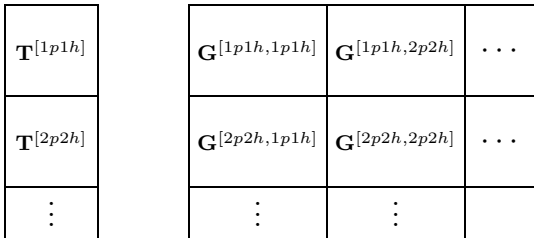

FIG. 6: Block structure of the vectors $\mathbf{T}$ and the matrices $\mathbf{G}$

Note that this expression for $R^{(I)}$ holds in general, not just in perturbation theory, and thus could serve as a starting point for approximation schemes like e.g. the Algebraic Diagrammatic Construction scheme [1, 27, 30].

The vectors $\mathbf{T}$ and the matrices $\mathbf{G}$, $\mathbf{E}$ and $\mathbf{V}$ can be subdivided into blocks by considering the different possible classes of excitations separately (see Fig. 6). In the following, we will label these blocks with the superscripts 1, 2, etc., enclosed in square brackets, i. e. $\mathbf{T}^{[1]}_{tu}$ refers to the generalized densities between $1p1h$ states and the ground state. This enables us to write the decomposition of R in first order in the following way:

$$
\begin{aligned}
R^{(I)(1)}_{pqrstu}(\omega_f,\omega_i,\omega) \;=\; & \mathbf{T}^{[1](1)\dagger}_{qp}\frac{1}{\omega_f-\mathbf{E}^{[1]}}\mathbf{G}^{[1,1](0)}_{rs}(\omega)\frac{1}{\omega_i-\mathbf{E}^{[1]}}\mathbf{T}^{[1](0)}_{tu} \\
&+\mathbf{T}^{[1](0)\dagger}_{qp}\frac{1}{\omega_f-\mathbf{E}^{[1]}}\mathbf{G}^{[1,1](0)}_{rs}(\omega)\frac{1}{\omega_i-\mathbf{E}^{[1]}}\mathbf{T}^{[1](1)}_{tu} \\
&+\mathbf{T}^{[2](1)\dagger}_{qp}\frac{1}{\omega_f-\mathbf{E}^{[2]}}\mathbf{G}^{[2,1](0)}_{rs}(\omega)\frac{1}{\omega_i-\mathbf{E}^{[1]}}\mathbf{T}^{[1](1)}_{tu} \\
&+\mathbf{T}^{[1](0)\dagger}_{qp}\frac{1}{\omega_f-\mathbf{E}^{[1]}}\mathbf{G}^{[1,2](0)}_{rs}(\omega)\frac{1}{\omega_i-\mathbf{E}^{[2]}}\mathbf{T}^{[2](1)}_{tu} \\
&+\mathbf{T}^{[1](0)\dagger}_{qp}\frac{1}{\omega_f-\mathbf{E}^{[1]}}\mathbf{G}^{[1,1](1)}_{rs}(\omega)\frac{1}{\omega_i-\mathbf{E}^{[1]}}\mathbf{T}^{[1](0)}_{tu} \\
&+\mathbf{T}^{[1](0)\dagger}_{qp}\frac{1}{\omega_f-\mathbf{E}^{[1]}}\mathbf{V}^{[1](1)}\frac{1}{\omega_f-\mathbf{E}^{[1]}}\mathbf{G}^{[1,1](0)}_{rs}(\omega)\frac{1}{\omega_i-\mathbf{E}^{[1]}}\mathbf{T}^{[1](0)}_{tu} \\
&+\mathbf{T}^{[1](0)\dagger}_{qp}\frac{1}{\omega_f-\mathbf{E}^{[1]}}\mathbf{G}^{[1,1](0)}_{rs}(\omega)\frac{1}{\omega_i-\mathbf{E}^{[1]}}\mathbf{V}^{[1](1)}\frac{1}{\omega_i-\mathbf{E}^{[1]}}\mathbf{T}^{[1](0)}_{tu}.
\end{aligned}
\tag{33}
$$

Evaluating the diagrams in Fig. 4, one can determine their contributions to each of the seven terms above. The explicit results can be found in appendix 1. It turns out that the first term gets contributions from the diagrams $3c, 3d, 4c, 4d$, the second from $5b, 5d, 6b, 6d$, the third from $1c, 1d, 2c, 2d, 5c, 5d, 6c, 6d$, the fourth from $1b-4b, 1e-4e$, the fifth from $1a-6a, 1b-6b, 1c-6c$, the sixth from $3c, 4c$, and the seventh from the diagrams $5b, 6b$.

We are interested here only in the fifth term, which contains the first order contribution

to the inelastic propagator between $1p-1h$ states. The propagator for the ground state has no contribution in first order, but the energy difference occuring in its argument (compare equation (26)) has a first order contribution, and hence this term has also to be taken into account. We then finally obtain:

$$\begin{aligned}
G_{qr}^{+n[q\bar{p},t\bar{u}](1)} &= \frac{\bar{n}_r}{\omega+\epsilon_p-\epsilon_q-\epsilon_r+i0^+}\Big[-n_s v_{qrst}\delta_{pu}+n_s v_{rups}\delta_{qt}+n_s v_{uqps}\delta_{rt} \\
&\quad -n_s v_{rqpt}\delta_{su}-\bar{n}_s v_{urpt}\delta_{qs}\left(1-\delta_{pu}\delta_{rt}\right)\Big]+\frac{n_r n_s v_{uqst}\delta_{pr}\left(1-\delta_{qt}\delta_{su}\right)}{\omega-\epsilon_q+i0^+} \\
&+ \frac{\bar{n}_s}{\omega-\epsilon_s-\epsilon_t+\epsilon_u+i0^+}\Big[n_r v_{qrst}\delta_{pu}-n_r v_{rups}\delta_{qt}-n_r v_{urpt}\delta_{qs} \\
&\quad +n_r v_{uqst}\delta_{pr}+\bar{n}_r v_{uqps}\delta_{rt}\left(1-\delta_{pu}\delta_{qs}\right)\Big]-\frac{n_r n_s v_{rqpt}\delta_{su}\left(1-\delta_{pr}\delta_{qt}\right)}{\omega-\epsilon_t+i0^+} \\
&+ \bar{n}_r\bar{n}_s\frac{-V_{qr[st]}\delta_{pu}+V_{ru[ps]}\delta_{qt}+V_{uq[ps]}\delta_{rt}+V_{ur[pt]}\delta_{qs}}{(\omega+\epsilon_p-\epsilon_q-\epsilon_r+i0^+)(\omega-\epsilon_s-\epsilon_t+\epsilon_u+i0^+)} \\
&+ \frac{\bar{n}_r n_s V_{rq[pt]}\delta_{su}}{(\omega+\epsilon_p-\epsilon_q-\epsilon_r+i0^+)(\omega-\epsilon_t+i0^+)} \\
&+ \frac{n_r\bar{n}_s V_{uq[st]}\delta_{pr}}{(\omega-\epsilon_q+i0^+)(\omega-\epsilon_s-\epsilon_t+\epsilon_u+i0^+)} \\
&- \frac{\delta_{qt}\delta_{pu}\delta_{rs}\bar{n}_s}{\omega+\epsilon_p-\epsilon_q-\epsilon_r-V_{pq[pq]}+i0^+}
\end{aligned} \tag{34}$$

Here the abbreviation

$$v_{abcd}=\frac{V_{ab[cd]}}{\epsilon_a+\epsilon_b-\epsilon_c-\epsilon_d} \tag{35}$$

was introduced.

The arguments used above can be generalized to higher orders. It turns out that a diagram of order n which has an internal vertex at a time before t_i or after t_f can not contribute to $\mathbf{G}^{[1,1](n)}$. Hence if one is only interested in the inelastic propagators between $1p-1h$ states, one does not need to evaluate such diagrams. This leads to a considerable reduction in the number of time orderings: only $(n+2)!/2$ (=1, 3, 12, ...) Goldstone diagrams are necessary to evaluate every Feynman diagram and any given time ordering of the external vertices, i.e. 2 diagrams in zeroth order, 18 in first order, and 432 in second order. In contrast, if one is also interested in propagators between higher excited states, all $(n+4)!/4!$ time orderings have to be considered.

For determining $G^{-n[M,N]}$ and the other inelastic Green's functions, one can construct the diagrams for $R^{(II)}$ to $R^{(IV)}$ in an analogous way. The evaluation of the diagrams is very similar; one can express $R^{(II)}$ to $R^{(IV)}$ using a matrix notation like that used for $R^{(I)}$ in (32).

The only difference is that one has to pay special attention to the additional phase factors appearing in $R^{(II)}(\omega_f, \omega_i, \tau)$ and $R^{(III)}(\omega_f, \omega_i, \tau)$ [see eqs.(11) and (12)]. These lead to a shift in the variable ω of the Fourier-transformed quantities $R^{(II)}(\omega_f, \omega_i, \omega)$ and $R^{(III)}(\omega_f, \omega_i, \omega)$ which are obtained by evaluating the diagrams. A closer analyis reveals that one has to define the matrix $\mathbf{G}_{rs}(\omega)$ in (32) differently. The matrices now have the elements

$$G_{rs}^{-s[M,N]}\left(\omega - \omega_f - \omega_i + \left(E^{[M]} - E^{[0]}\right) + \left(E^{[N]} - E^{[0]}\right)\right)$$
$$-\delta_{MN} G_{rs}^{-[0,0]}\left(\omega - \omega_f - \omega_i + \left(E^{[N]} - E^{[0]}\right)\right)$$

and

$$G_{rs}^{+i[M,N]}\left(\omega - \omega_i - \omega_f - \left(E^{[M]} - E^{[0]}\right) - \left(E^{[N]} - E^{[0]}\right)\right)$$
$$-\delta_{MN} G_{rs}^{-[0,0]}\left(\omega - \omega_f - \omega_i - \left(E^{[N]} - E^{[0]}\right)\right),$$

respectively. In $R^{(IV)}$, no additional phase factors appear, so that the matrix there has simply the elements

$$G_{rs}^{-n[M,N]}(\omega) - \delta_{MN} G_{rs}^{-[0,0]}\left(\omega + (E^{[M]} - E^{[0]})\right)$$

So from the viewpoint of the actual diagrammatic evaluation, the natural inelastic Green's function indeed seems to be more "natural".

C. Closed-shell anion

1. *Expressing the inelastic propagator by elastic quantities*

Here we use the four-point, four-times Green's function which is defined with respect to the ground state $|0^->$ of the (closed-shell) anion:

$$\begin{aligned} iR_{pqrs}(t_f, t, t', t_i) \;=\; & - < 0^- | \hat{T}\left[c_p^\dagger(t_f) c_q(t) c_r^\dagger(t') c_s(t_i)\right] |0^- > \\ & + < 0^- | \hat{T}\left[c_p^\dagger(t_f) c_s(t_i)\right] |0^- >< 0^- | \hat{T}\left[c_q(t) c_r^\dagger(t')\right] |0^- > . \end{aligned} \tag{36}$$

The extra factor consisting of a product of two-times Green's function is added to eliminate the disjoint diagrams in the diagrammatic expansion (see Fig. 7).

This four-times Green's function is essentially identical to the particle-hole response function [29]. A well-known special case of that function, with only two different time arguments

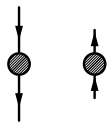

FIG. 7: Disjoint diagrams which do not contribute to the four-times Green's function for a closed-shell anion

instead of the four in the general form, is the polarization propagator. Since that propagator and the Green's function we discuss here differ in the number of their different time arguments only, the Feynman diagrams for both are essentially identical, but the Goldstone diagrams are different.

Again, there are 24 different time orderings possible here, which all depend only on the three time differences $\tau_f = t_f - t$, $\tau = t - t'$ and $\tau_i = t' - t_i$; hence we can write:

$$\begin{aligned} R_{pqrs}(t_f, t, t', t_i) &= \theta(\tau_f)\theta(\tau)\theta(\tau_i) R^{(I)}_{pqrs}(\tau_f, \tau, \tau_i) \\ &+ \theta(\tau_f)\theta(-\tau)\theta(\tau_i) R^{(II)}_{pqrs}(\tau_f, \tau, \tau_i) \\ &+ \ldots \end{aligned}$$

The other 22 time orderings not explicitly shown give contributions which are not of interest here.

The steps we use here to establish the connections with the various inelastic Green's functions are very similar to those in the previous section. First, we insert complete sets of energy eigenstates $|N>$ (here not of the anion itself, but of the neutral open-shell molecule of interest), and subsequently we use the time dependence of the destruction and creation operators to obtain

$$\begin{aligned} R^{(I)}_{pqrs}(\tau_f, t, t', \tau_i) &= -\sum_{M,N} x_p^{[M]\dagger} x_s^{[N]} e^{-i(E^{[M]} - E^{[0^-]})\tau_f} e^{-i(E^{[N]} - E^{[0^-]})\tau_i} \\ &\cdot e^{-i(E^{[M]} - E^{[0^-]})t)} e^{i(E^{[M]} - E^{[0^-]})t')} \\ &\cdot \left(< M|c_q(t) c_r^\dagger(t')|N > - \delta_{MN} < 0^-|c_q(t) c_r^\dagger(t')|0^- > \right), \end{aligned}$$

where $E^{[0^-]}$ denotes the ground state energy of the closed-shell anion, $E^{[M]}$ the possible energies of the neutral open-shell molecule, and the transition amplitudes

$$x_s^{[N]} = < N|c_s|0^- > \tag{37}$$

were introduced. By using a slightly different definition for the phase factor for the natural Green's function,

$$\Phi^{+n[M,N]}(t,t') = -(E^{[M]} - E^{[0^-]})t + (E^{[N]} - E^{[0^-]})t' \tag{38}$$

i. .e. replacing the energy differences to the ground state of the neutral molecule with energy differences to the ground state of the anion, we can write the first time ordering $R^{(I)}$ as

$$\begin{aligned} R^{(I)}_{pqrs}(\tau_f,\tau,\tau_i) \;=\; & -\sum_{M,N} x_p^{[M]\dagger} x_s^{[N]} e^{-i(E^{[M]}-E^{[0^-]})\tau_f} e^{-i(E^{[N]}-E^{[0^-]})\tau_i} \\ & \cdot \left(G_{qr}^{+n[M,N]}(\tau) - \delta_{MN} G_{qr}^{+[0^-,0^-]}(\tau) e^{-i(E^{[M]}-E^{[0^-]})\tau)} \right), \end{aligned} \tag{39}$$

where $G^{+[0^-,0^-]}$ is the propagator for the ground state of the anion. Note that due to the changed phase factor, the poles of the particle component of the inelastic propagator $G^{+n[M,N]}$ are no longer the electron attachment energies of the neutral molecule, but instead excitation energies of the anion.

Fourier transforming of $R^{(I)}$ with respect to τ_f and τ_i gives now:

$$\begin{aligned} R^{(I)}_{pqrs}(\omega_f,\omega_i,\tau) \;=\; & \sum_{M,N} \frac{x_p^{[M]\dagger}}{\omega_f - (E^{[M]} - E^{[0^-]}) + i0^+} \frac{x_s^{[N]}}{\omega_i - (E^{[N]} - E^{[0^-]}) + i0^+} \\ & \cdot \left(G_{qr}^{+n[M,N]}(\tau) - \delta_{MN} G_{qr}^{+[0^-,0^-]}(\tau) e^{-i(E^{[M]}-E^{[0^-]})\tau)} \right). \end{aligned} \tag{40}$$

The poles of this Green's function (in both ω_f and ω_i) are given by the energy differences of the excited states of the neutral open-shell molecule to the ground state of the anion (i. e. by the ionization energies of the anion), and the residues of the double poles are

$$x_p^{[M]\dagger} \left(G_{qr}^{+n[M,N]}(\tau) - \delta_{MN} G_{qr}^{+[0^-,0^-]}(\tau) e^{-i(E^{[M]}-E^{[0^-]})\tau)} \right) x_s^{[N]}. \tag{41}$$

Again, as in the preceding section one determines the particle component of the natural Green's function for inelastic scattering from the residues of a higher Green's function. Since here the sums over M and N include the ground state of the neutral molecule, it is possible in principle to determine also the elastic propagator for the (open-shell!) neutral molecule. Actually, what one obtains for $M = N = 0$ is the elastic propagator times the phase factor

$$e^{-(E^{[0]}-E^{[0^-]})\tau},$$

arising from the slightly different phase definition introduced above in eq.(38).

Similarly, one obtains the second part of R, which corresponds to the second time ordering. As found for the closed-shell molecule in section II B, it turns out that $R^{(II)}$ gives the hole component of the scattering-motivated inelastic Green's function (provided that in the phase factor $\Phi^{-s[M,N]}$, the energy differences to the ground state of the anion are used):

$$R^{(II)}_{pqrs}(\omega_f,\omega_i,t,t') = \sum_{M,N} \frac{x_p^{[M]\dagger} e^{-i(\omega_f-(E^{[M]}-E^{[0^-]}))\tau}}{\omega_f-(E^{[M]}-E^{[0^-]})+i0^+} \frac{x_s^{[N]} e^{-i(\omega_i-(E^{[N]}-E^{[0^-]}))\tau}}{\omega_i-(E^{[N]}-E^{[0^-]})+i0^+} \cdot \left(G^{-s[M,N]}_{qr}(t,t') - \delta_{MN} G^{-[0^-,0^-]}_{qr}(t,t') e^{-i(E^{[M]}-E^{[0^-]})\tau)} \right). \qquad (42)$$

Because of the phase convention used, the poles of the particle component of the inelastic propagator $G^{+s[M,N]}$ are now not the ionization energies of the neutral molecule, but the double ionization energies of the anion.

We see that $R^{(I)}$ and $R^{(II)}$ taken together determine the scattering-motivated inelastic Green's function, just as we have found in the preceding section. But, in contrast to the situation there, the hole component of the natural inelastic Green's function (and therefore also the ionization-motivated Green's function) can not be obtained here from the time-orderings three and four, since these time-orderings involve intermediate states of the dianion rather than those of the neutral molecule.

Nevertheless, one can obtain the ionization-motivated inelastic Green's function if one uses alternatively the time differences $\tau'_f = t_f - t'$ and $\tau'_i = t - t_i$ instead of τ_f and τ_i. Then, $R^{(I)}$ gives the particle component of the ionization-motivated Green's function and $R^{(II)}$ gives the hole component of the natural Green's function—and hence $R^{(I)}$ and $R^{(II)}$ determine the whole ionization-motivated inelastic Green's function.

2. Evaluation by diagrams

The Feynman rules for the four-times Green's function are very similar to those discussed in some detail for the closed-shell molecule (see section II B). The differences are: one has now only $2n+2$ instead of $2n+3$ directed free Green's function lines in rule (F1) (at the time z_i, there is now only a line which ends there, and at time t_f, only a line which starts there), resulting in an overall factor of i^{n-1} instead of i^n in rule (F4). However, the factor $+1$ for the Goldstone diagrams in rule (G4) stays the same, since one still has the same number of vertices and hence the same number of cuts. The additional sign factor in rules (F4) and

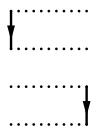

FIG. 8: Goldstone diagram for the first component $R^{(I)}$ of the four-times Green's function for a closed-shell anion in zeroth order

(G4) arising from the way in which the external times t_f, t, t' and t_i are connected is here -1 if t_f is connected to t_i and $+1$ otherwise.

The number of Feynman diagrams is considerably lower here: In order n (Abrikosov notation), one has now only

- $n = 0$: 1
- $n = 1$: 1
- $n = 2$: 5

The Feynman diagrams arising here are similar to the ones for the polarization propagator (which are shown up to second order e. g. in [27]). One crucial difference is that here, for a given time ordering of the external vertices in order n one has to consider $(n+4)!/4!$ different Goldstone diagrams for every Feynman diagram. The number of Goldstone diagrams for a given time ordering of the external vertices in order n (Abrikosov notation) is then:

- $n = 0$: 1 (Fig. 8)
- $n = 1$: 5 (Fig. 9)
- $n = 2$: 150

For the second order, the five Feynman diagrams are shown in Fig. 10.

In leading order, the single diagram of Fig. 8 can be easily evaluated to give

$$R^{(I)(0)}_{pqrs} = \frac{n_p \delta_{pq}}{\omega + \epsilon_p + i0^+} \frac{1}{\omega + i0^+} \frac{n_s \delta_{rs}}{\omega + \epsilon_s + i0^+}. \tag{43}$$

Taking also the elastic propagator $G^{+[0^-,0^-]}$ for the ground state of the anion into account, one obtains

$$x_s^{[\bar{s}](0)} \;=\; n_s \tag{44}$$

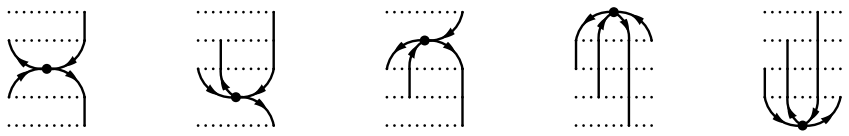

FIG. 9: Goldstone diagrams for the first component $R^{(I)}$ of the four-times Green's function for a closed-shell anion in first order

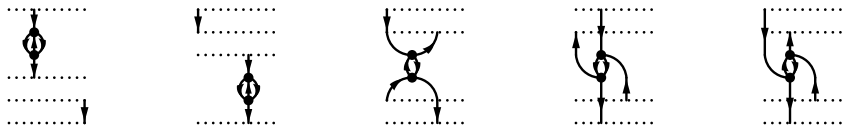

FIG. 10: Feynman diagrams for the four-times Green's function for a closed-shell anion in second order

$$\left(E^{[\bar{s}]} - E^{[0^-]}\right)^{(0)} = -\epsilon_s \tag{45}$$

$$G^{+n[\bar{p},\bar{s}](0)}_{qr}(\omega) = \frac{\delta_{pq}\delta_{rs}}{\omega + i0^+} - \delta_{ps}\frac{\bar{n}_r\delta_{qr}}{\omega - (\epsilon_r - \epsilon_s) + i0^+}, \tag{46}$$

again in agreement with the results one can obtain by a direct perturbative evaluation. We wrote here $\bar{p}$ for a hole state of the anion.

To evaluate the first order, one can introduce vectors $\mathbf{X}_s$ containing the transition amplitudes $< N|c_s|0^- >$ for *fixed* s, and matrices $\mathbf{G}_{qr}$, $\mathbf{E}$ and $\mathbf{V}$, analogously to the case of the closed-shell molecule (compare section II B). These matrices can be subdivided into blocks again, this time for the $1h$, $2h-1p$, etc. excitations. We denote them again with superscripts 1, 2, etc. in square brackets. This enables us to write:

$$\begin{aligned} R^{(I)(1)}_{pqrs}(\omega_f,\omega_i,\omega) = {} & \mathbf{X}^{[1](1)\dagger}_p \frac{1}{\omega_f - \mathbf{E}^{[1]}} \mathbf{G}^{[1,1](0)}_{qr}(\omega) \frac{1}{\omega_i - \mathbf{E}^{[1]}} \mathbf{X}^{[1](0)}_s \\ & + \mathbf{X}^{[1](0)\dagger}_p \frac{1}{\omega_f - \mathbf{E}^{[1]}} \mathbf{G}^{[1,1](0)}_{qr}(\omega) \frac{1}{\omega_i - \mathbf{E}^{[1]}} \mathbf{X}^{[1](1)}_s \\ & + \mathbf{X}^{[2](1)\dagger}_p \frac{1}{\omega_f - \mathbf{E}^{[2]}} \mathbf{G}^{[2,1](0)}_{qr}(\omega) \frac{1}{\omega_i - \mathbf{E}^{[1]}} \mathbf{X}^{[1](0)}_s \\ & + \mathbf{X}^{[1](0)\dagger}_p \frac{1}{\omega_f - \mathbf{E}^{[1]}} \mathbf{G}^{[1,2](0)}_{qr}(\omega) \frac{1}{\omega_i - \mathbf{E}^{[2]}} \mathbf{X}^{[2](1)}_s \\ & + \mathbf{X}^{[1](0)\dagger}_p \frac{1}{\omega_f - \mathbf{E}^{[1]}} \mathbf{G}^{[1,1](1)}_{qr}(\omega) \frac{1}{\omega_i - \mathbf{E}^{[1]}} \mathbf{X}^{[1](0)}_s \end{aligned} \tag{47}$$

$$+\mathbf{X}_p^{[1](0)\dagger}\frac{1}{\omega_f-\mathbf{E}^{[1]}}\mathbf{V}^{[1](1)}\frac{1}{\omega_f-\mathbf{E}^{[1]}}\mathbf{G}_{qr}^{[1,1](0)}(\omega)\frac{1}{\omega_i-\mathbf{E}^{[1]}}\mathbf{X}_s^{[1](0)}$$
$$+\mathbf{X}_p^{[1](0)\dagger}\frac{1}{\omega_f-\mathbf{E}^{[1]}}\mathbf{G}_{qr}^{[1,1](0)}(\omega)\frac{1}{\omega_i-\mathbf{E}^{[1]}}\mathbf{V}^{[1](1)}\frac{1}{\omega_i-\mathbf{E}^{[1]}}\mathbf{X}_s^{[1](0)},$$

i. e. there are seven terms contributing to $R^{(I)}$ in first order. Analysing the diagrams of Fig. 9, it turns out that there are no contributions to the first two and the last two terms (i. e. the transition amplitudes to the $1h$ excitations and the energies of these excitations receive no first order contribution in perturbation theory). The third term gets contributions from the third and fourth diagram, the fourth term from the second and fifth diagram, and the fifth from the first three diagrams. The explicit results are listed in appendix 2.

We are interested here only in the fifth term, since only this term contains the first order contribution to the inelastic Green's function. Taking the results from all three relevant diagrams together and considering that the propagator for the ground state has no contribution in first order, we finally obtain:

$$G_{qr}^{+n[\bar{p},\bar{s}](1)} = v_{qspr}\left[\frac{\bar{n}_q}{\omega-(\epsilon_q-\epsilon_p)+i0^+}-\frac{\bar{n}_r}{\omega-(\epsilon_r-\epsilon_s)+i0^+}\right]. \tag{48}$$

One achieves a significant reduction in the necessary number of diagrams if one is only interested in the propagators between $1h$ states. In this case, only $(n+2)!/2$ time orderings have to be considered. This leads per Feynman diagram to 1 Goldstone diagram in zeroth order, 3 in first order, and to only 60 in second order. To evaluate these diagrams is a very feasible task. Even the third order, which involves 23 Feynman diagrams (which are very similar to the 23 Feynman diagrams for the polarization propagator in third order [30]) and 60 time orderings, and hence 1380 vGoldstone diagrams, could be viable.

D. Closed-shell cation

1. *Expressing the inelastic propagator by elastic quantities*

This case is very similar to the case of the closed-shell anion, and we can keep the discussion short. We have to use the following four-point, four-times Green's function here:

$$\begin{aligned} iR_{pqrs}(t_f,t,t',t_i) \;=\; &-<0^+|\hat{T}\left[c_p(t_f)c_q(t)c_r^\dagger(t')c_s^\dagger(t_i)\right]|0^+> \\ &+<0^+|\hat{T}\left[c_p(t_f)c_s^\dagger(t_i)\right]|0^+><0^+|\hat{T}\left[c_q(t)c_r^\dagger(t')\right]|0^+>. \end{aligned} \tag{49}$$

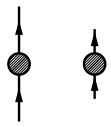

FIG. 11: Disjoint diagrams which do not contribute to the four-times Green's function for a closed-shell cation

$|0^+>$ denotes the ground state of the (closed-shell) cation, the remaining notation is identical to that in the previous sections. The disjoint diagrams which are subtracted here are shown in Fig. 11.

In complete analogy to the preceding sections, we obtain

$$R^{(I)}_{pqrs}(\omega_f,\omega_i,\tau) = \sum_{M,N} \frac{y_p^{[M]\dagger}}{\omega_f-(E^{[M]}-E^{[0^+]})+i0^+} \frac{y_s^{[N]}}{\omega_i-(E^{[N]}-E^{[0^+]})+i0^+} \cdot\left(G^{+[M,N]}_{qr}(\tau)-\delta_{MN}G^{+[0^+,0^+]}_{qr}(\tau)e^{-i(E^{[M]}-E^{[0^+]})\tau)}\right) \quad (50)$$

and

$$R^{(II)}_{pqrs}(\omega_f,\omega_i,\tau) = \sum_{M,N} \frac{y_p^{[M]\dagger}e^{-i(\omega_f-(E^{[M]}-E^{[0^+]}))\tau}}{\omega_f-(E^{[M]}-E^{[0^+]})+i0^+} \frac{y_s^{[N]}e^{-i(\omega_i-(E^{[N]}-E^{[0^+]}))\tau}}{\omega_i-(E^{[N]}-E^{[0^+]})+i0^+} \cdot\left(G^{-[M,N]}_{qr}(\tau)-\delta_{MN}G^{-[0^+,0^+]}_{qr}(\tau)e^{-i(E^{[M]}-E^{[0^+]})\tau)}\right), \quad (51)$$

for the Fourier transforms of the first and second time orderings. $E^{[0^+]}$ denotes the ground state energy of the closed-shell cation, $E^{[M]}$ the possible energies of the neutral open-shell molecule, $G^{[0^+,0^+]}$ is the propagator for the ground state of the cation, and the transition amplitudes are

$$y_s^{[N]} =< N|c_s^\dagger|0^+> . \quad (52)$$

The phase factors one has to use here include the energy differences to the ground state of the cation. All the remarks of the previous section with respect to the changed meanings of the poles apply here also.

Again, the two time orderings $R^{(I)}$ and $R^{(II)}$ taken together give the scattering-motivated inelastic Green's function. And again, one can also obtain the elastic Green's function for the ground state of the neutral, *open-shell* molecule (times a phase factor), just as in the investigation of the closed-shell anion in section II C. Similarly, the hole component of the natural inelastic Green's function and the ionization-motivated Green's function can not be obtained from the time-orderings $R^{(III)}$ and $R^{(IV)}$, since these time-orderings involve

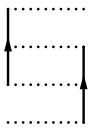

FIG. 12: Goldstone diagram for the first component $R^{(I)}$ of the four-times Green's function for a closed-shell cation in zeroth order

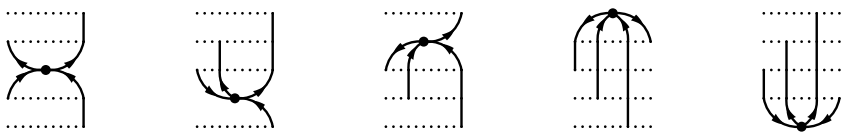

FIG. 13: Goldstone diagrams for the first component $R^{(I)}$ of the four-times Green's function for a closed-shell cation in first order

intermediate states of the dication instead of those of the neutral molecule. This can be remedied by using alternatively the time differences $\tau'_f = t_f - t'$ and $\tau'_i = t - t_i$ in $R^{(I)}$ and $R^{(II)}$, as done in the preceding section.

2. Evaluation by diagrams

The Feynman rules to evaluate the elastic four-times Green's function are almost the same as those discussed for the closed-shell anion case (see section II C): in rule (F1), there is now a line starting at time t_i and a line ending at t_f, and the additional sign factor in rules (F4) and (G4) arising from the way in which the external times are connected is exactly the other way around, i.e. $+1$ if t_f and t_i are connected and -1 otherwise. The number of Feynman diagrams in nth order is identical to that in the preceding section. Also the appearance of these diagrams is very similar; in many of them, only the direction of two lines has to be changed. The Goldstone diagrams of zeroth and first order are shown in Figs. 12 and 13, and the Feynman diagrams of second order are shown in Fig. 14.

By evaluating the diagrams in the same way as for the anion, one obtains here for the particle component of the natural inelastic Green's function for the transitions between the

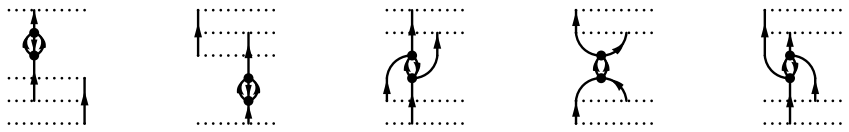

FIG. 14: Feynman diagrams for the four-times Green's function for a closed-shell cation in second order

$1p$ states $|p>$ and $|s>$ up to first order:

$$G_{qr}^{+n[p,s](0,1)}(\omega) = \frac{\delta_{pr}\delta_{qs}}{\omega-\epsilon_p-\epsilon_s+i0^+} - \delta_{ps}\frac{\bar{n}_r}{\omega-(\epsilon_r+\epsilon_s)+i0^+} + v_{qprs}\left[\frac{\bar{n}_q}{\omega-\epsilon_p-\epsilon_q+i0^+} - \frac{\bar{n}_r}{\omega-\epsilon_r-\epsilon_s+i0^+}\right]. \quad (53)$$

It is obvious by now that starting with a suitable elastic higher Green's function of a closed-shell anion or cation, the determination of the inelastic Green's function for the molecule is much easier than in the case where the neutral molecule itself is closed-shell. A slight drawback of this method is that all excited states are written with respect to the ion. In many cases, these states are of interest by themselves, however.

III. CALCULATION OF THE INELASTIC PROPAGATOR VIA THE GENERALIZED ONE-PARTICLE DENSITY

A. Dyson-like equations for the inelastic propagator

The approach outlined in section II for obtaining the inelastic Green's function is nice from a mathematical point of view, since it gives the Green's function directly. Additionally, it reveals the significance of the scattering-motivated and the ionization-motivated Green's function, and could help in the physical interpretation of the three different definitions for the inelastic Green's function.

However, this approach looks quite tedious - the number of Goldstone diagrams (and even of the Feynman diagrams) one has to consider grows very rapidly with the order n, and already the second order poses a considerable challenge. Hence the derivation of other methods, which might be more practical, is desirable. We will outline such an alternative in this section.

As has been shown in [21], one can write the following equation of motion for the inelastic Green's function:

$$\begin{aligned}\left[i\frac{d}{dt}-\epsilon_p\right]G_{pq}^{[M,N]}(t,t') \;=\; & \delta(t-t')\delta_{pq}\delta_{MN}+\sum_k W_{pk}G_{kq}^{[M,N]}(t,t') \\ & +\frac{1}{2}\sum_{n,k,l} V_{pn[kl]}G_{nlk,q}^{[M,N]}(t,t') \\ & -G_{pq}^{+[M,N]}(t,t')\left(-(E^{[M]}-E^{[0]})+f^{+[M,N]}\right) \\ & -G_{pq}^{-[M,N]}(t,t')\left((E^{[N]}-E^{[0]})+f^{-[M,N]}\right)\end{aligned} \tag{54}$$

with

$$\begin{aligned}iG_{nlk,q}^{[M,N]}(t,t') \;=\; & \theta(t-t')<M|c_n^\dagger(t)c_l(t)c_k(t)c_q^\dagger(t')|N>e^{i\Phi^{+[M,N]}(t,t')} \\ & -\theta(t'-t)<M|c_q^\dagger(t')c_n^\dagger(t)c_l(t)c_k(t)|N>e^{i\Phi^{-[M,N]}(t,t')}.\end{aligned} \tag{55}$$

As we have seen in the direct approach (sections II C and II D), it is convenient to replace the ground state energy $E^{[0]}$ of the neutral molecule with the ground state energy $E^{[0^\pm]}$ of the corresponding ion if one treats the case of a closed-shell anion or cation. In the following, we will assume for simplicity of notation that $E^{[0]}$ stands for the relevant ground state energy.

It suffices to investigate the equation of motion for the natural inelastic Green's function (for which it simplifies considerably, since the factors f^+ and f^- are zero there), since any other inelastic Green's function can be obtained from it by

$$G_{pq}^{\pm[M,N]}(\tau)=G_{pq}^{\pm n[M,N]}(\tau)\,e^{if^{\pm[M,N]}\tau}$$

or, for the Fourier transforms,

$$G_{pq}^{\pm[M,N]}(\omega)=G_{pq}^{\pm n[M,N]}\left(\omega+f^{\pm[M,N]}\right).$$

For reasons which will soon become clear, it is necessary to treat the equations of motion for the particle and the hole component separately (see also [22]). The particle component of the higher Green's function $G_{nlk,q}^{[M,N]}$ appearing in the equations of motion can be rewritten by inserting a complete set of eigenstates and using the usual time dependence of the destruction and creation operators:

$$\begin{aligned}iG_{nlk,q}^{+[M,N]}(t,t') \;=\; & \theta(t-t')\sum_P \rho_{nl}^{[M,P]}e^{i(E^{[M]}-E^{[P]})t}<P|c_k(t)c_q^\dagger(t')|N>e^{i\Phi^{+[M,N]}(t,t')} \\ =\; & \sum_P \rho_{nl}^{[M,P]}iG_{kq}^{+n[P,N]}(t,t').\end{aligned} \tag{56}$$

If one also wants to express in a similar way the hole component G^- by generalized densities, one first has to commute the operators $c_n^\dagger$ and c_l. However, this gives a factor δ_{nl}, and that yields in the equation of motion a term with

$$\sum_n V_{pn[kn]},$$

which *diverges*. Hence one has to treat the case $n = l$ separately. One finally arrives at

$$\begin{aligned} iG^{-[M,N]}_{nlk,q}(t,t') \;=\; \sum_P \Big(& -iG^{-n[M,P]}_{lq}(t,t')\rho^{[P,N]}_{nk}(1-\delta_{nl}) - iG^{-n[M,N]}_{nq}(t,t')\delta_{nl}\delta_{nk} \\ & + iG^{-n[M,P]}_{kq}(t,t')\delta_{nl}\rho^{[P,N]}_{nn}\Big). \end{aligned} \tag{57}$$

Note that the second term on the right hand side does not contribute in the equation of motion (54), since it leads to a term $V_{pn[nn]} = 0$ in the sum

$$\sum_{n,k,l} V_{pn[kl]} G^{-[M,N]}_{nlk,q}(t,t').$$

By introducing the abbreviations

$$\begin{aligned} A^{+[M,P]}_{pk} \;&=\; W_{pk}\delta_{MP} + \frac{1}{2}\sum_{nl} V_{pn[kl]}\rho^{[M,P]}_{nl}, \\ A^{-[P,N]}_{pk} \;&=\; W_{pk}\delta_{PN} + \frac{1}{2}\sum_{n,l;\,n\neq k} V_{pn[kl]}\rho^{[P,N]}_{nl} + \frac{1}{2}\sum_n V_{pn[kn]}\rho^{[P,N]}_{nn}, \end{aligned} \tag{58}$$

we then arrive at the following simplified expressions for the equations of motion for the particle component

$$\begin{aligned} & \left\{ i\frac{d}{dt} - \left[\epsilon_p + (E^{[M]} - E^{[0]})\right]\right\} G^{+n[M,N]}_{pq}(t,t') \\ =\; & \delta(t-t')\rho^{+[M,N]}_{pq} + \sum_P \sum_k A^{+[M,P]}_{pk} G^{+n[P,N]}_{kq}(t,t') \end{aligned} \tag{59}$$

and the hole component

$$\begin{aligned} & \left\{ i\frac{d}{dt} - \left[\epsilon_p - (E^{[N]} - E^{[0]})\right]\right\} G^{-n[M,N]}_{pq}(t,t') \\ =\; & \delta(t-t')\rho^{[M,N]}_{qp} + \sum_P \sum_k A^{-[P,N]}_{pk} G^{-n[M,P]}_{kq}(t,t') \end{aligned} \tag{60}$$

of the natural inelastic propagator, where

$$\rho^{+[M,N]}_{pq} =< M|c_p c_q^\dagger|N > .$$

The equation of motion for G^{-n} now only contains the "advanced type" quantities G^{-n} and ρ. Note that by treating $G^{+n[M,N]}_{nlk,q}$ in a way analogous to $G^{-n[M,N]}_{nlk,q}$, one can obtain

$$\begin{aligned} iG^{+n[M,N]}_{nlk,q}(t,t') \;=\; \sum_P \Big(\rho^{+[M,P]}_{ln} - iG^{+n[P,N]}_{kq}(t,t')(1-\delta_{nl}) - iG^{+n[M,N]}_{nq}(t,t')\delta_{nl}\delta_{nk} \\ +\rho^{+[M,P]}_{kn} iG^{+n[P,N]}_{nq}(t,t')\delta_{nl}\Big) \end{aligned} \tag{61}$$

(again, in the equation of motion the term with δ_{nk} cancels out), and hence it is also possible to write an equation of motion for G^{+n} which only contains the "retarded type" quantities G^{+n} and ρ^{+}. Note that in [22], equations of motions for both components of the inelastic propagator were already given. But there, the problem of completely separating the two time-orderings of the propagator in the equations was left open.

Now it is convenient to Fourier transform equations (59) and (60), yielding:

$$\Big\{\omega - \Big[\epsilon_p + (E^{[M]} - E^{[0]})\Big]\Big\}\, G^{+n[M,N]}_{pq}(\omega) = \rho^{+[M,N]}_{pq} + \sum_P \sum_k A^{+[M,P]}_{pk} G^{+n[M,N]}_{kq}(\omega)$$

and

$$\Big\{\omega - \Big[\epsilon_p - (E^{[N]} - E^{[0]})\Big]\Big\}\, G^{-n[M,N]}_{pq}(\omega) = \rho^{[M,N]}_{qp} + \sum_P \sum_k A^{-[P,N]}_{pk} G^{-n[M,P]}_{kq}(\omega),$$

and to introduce the abbreviations

$$\begin{aligned} \tilde{G}^{+[M,N]}_{pq}(\omega) \;&=\; \frac{\delta_{pq}\delta_{MN}}{\omega - [\epsilon_p + (E^{[M]} - E^{[0]})] + i0^+}, \\ \tilde{G}^{-[M,N]}_{pq}(\omega) \;&=\; \frac{\delta_{pq}\delta_{MN}}{\omega - [\epsilon_p - (E^{[N]} - E^{[0]})] - i0^+}. \end{aligned} \tag{62}$$

$\tilde{\mathbf{G}}^{\pm}$ is *not* the lowest-order contribution to $\mathbf{G}^{\pm}$ (i. e. the contribution for no interactions between the electrons). In order to distinguish this propagator from the free one, it is denoted by a tilde here, contrary to the notation in [21], where a superscript (0) was used.

We arrive now at the following equations:

$$\begin{aligned} \sum_k \sum_P \Big[\Big(\tilde{G}^{+}\Big)^{-1}\Big]^{[M,P]}_{pk} G^{+n[P,N]}_{kq}(\omega) \;&=\; \rho^{+[M,N]}_{pq} + \sum_k \sum_P A^{+[M,P]}_{pk} G^{+n[P,N]}_{kq}(\omega) \\ \sum_k \sum_P \Big[\Big(\tilde{G}^{-}\Big)^{-1}\Big]^{[P,N]}_{pk} G^{-n[M,P]}_{kq}(\omega) \;&=\; \rho^{[M,N]}_{qp} + \sum_k \sum_P A^{-[P,N]}_{pk} G^{-n[M,P]}_{kq}(\omega). \end{aligned}$$

If one introduces super-matrices, it is easy to rewrite the first equation. But for the second equation, one has to interchange the order of the lower indices for $\tilde{G}^{-}$, G^{-} and A^{-}, i. e. we

define:

$$\begin{aligned}\left(\tilde{\mathbf{G}}^{-}\right)_{pq}^{[M,N]} &= \tilde{G}_{qp}^{-[M,N]} \\ \left(\mathbf{G}^{-}\right)_{pq}^{[M,N]} &= G_{qp}^{-n[M,N]} \\ \left(\mathbf{A}^{-}\right)_{pq}^{[M,N]} &= A_{qp}^{-[M,N]}.\end{aligned}$$

Then, the equations for G^+ and G^- can be written in a short, handy way:

$$\mathbf{G}^{+} = \tilde{\mathbf{G}}^{+}\boldsymbol{\rho}^{+} + \tilde{\mathbf{G}}^{+}\mathbf{A}^{+}\mathbf{G}^{+} \tag{63}$$

$$\mathbf{G}^{-} = \boldsymbol{\rho}\,\tilde{\mathbf{G}}^{-} + \mathbf{G}^{-}\mathbf{A}^{-}\tilde{\mathbf{G}}^{-}. \tag{64}$$

We have thus now arrived at Dyson-like equations for both components of the inelastic propagator. It should be remarked here that it is also possible to derive an equation of motion for G^- so that the order of the super-matrices in the Dyson-like equation for G^- is identical to the order in the one for G^+. This can be achieved by using

$$i\frac{d}{dt'}G_{pq}^{-[M,N]}(t,t') = -i\frac{d}{dt}G_{pq}^{-[M,N]}(t,t'),$$

which leads to

$$\left[i\frac{d}{dt} - \epsilon_q + E^{[M]} - E^{[0]}\right] G_{pq}^{-[M,N]}(t,t') = \delta(t-t')\rho_{qp}^{[M,N]} + \sum_k \sum_P A_{kq}^{[M,P]} G_{pk}^{-[P,N]}(t,t')$$

with

$$A_{kq}^{-[M,P]} = \delta_{MP} W_{kq} + \frac{1}{2}\sum_{mn;n\neq k} V_{mk[nq]}\rho_{mn}^{[M,P]} - \frac{1}{2}V_{kn[nq]}\rho_{nn}^{[M,P]}.$$

Fourier transforming and using the same super-matrix notation as above in (64) yields then the desired form

$$\mathbf{G}^{-} = \tilde{\mathbf{G}}^{-}\boldsymbol{\rho} + \tilde{\mathbf{G}}^{-}\mathbf{A}^{-}\mathbf{G}^{-}.$$

Finally we want to address the question of invertibility of the individual components of the inelastic Green's function. For the particle component, this was already discussed in [21]; the discussion here can proceed along the same lines. Using the Dyson-like equation (64), we can give an explicit expression for the hole component of the inelastic propagator:

$$\mathbf{G}^{-} = \boldsymbol{\rho}\left((\tilde{\mathbf{G}}^{-})^{-1} - \mathbf{A}^{-}\right).$$

If $\boldsymbol{\rho}$ were invertible, it would then follow that $\mathbf{G}^-$ is. But $\boldsymbol{\rho}$ is a singular matrix, which can be seen using the same argument as applied in [21] to $\boldsymbol{\rho}^+$: insert completeness between the

two operators in $\boldsymbol{\rho}$ and note that it then can be written as the matrix product $\boldsymbol{\rho} = \mathbf{a}^\dagger \mathbf{a}$, where $\mathbf{a}$ has the elements

$$a_{s,(qM)} =< s^+|b_q|M > .$$

Here, the states $|s^+>$ are the energy eigenstates of the molecule with one less electron. $\mathbf{a}$ is then a rectangular matrix with rank smaller than the dimension of $\boldsymbol{\rho}$. Therefore, the rank of $\boldsymbol{\rho}$ is smaller than its dimension, and consequently it is singular.

A crucial point concerning the Dyson-like equations (63) and (64) is that in order to calculate the inelastic Green's function, all one needs to know are the energies $E^{[M]}$ and the generalized densities $\rho_{pq}^{[M,N]}$ and $\rho_{pq}^{+[M,N]}$ of the target molecule. Since

$$\rho_{pq}^{[M,N]} + \rho_{qp}^{+[M,N]} = \delta_{MN}\delta_{pq}, \tag{65}$$

holds, calculating either ρ or ρ^+ suffices already.

We outline in the next three sections how one can obtain the generalized densities and the $E^{[M]}$, and from them the inelastic propagators. In analogy to the *direct approach*, the three cases of a closed-shell neutral molecule and closed-shell ions are separately discussed. We call the method of calculating the inelastic Green's function by using the generalized densities and the Dyson-like equations (63) and (64) the *Dyson approach* in the following.

B. Closed-shell molecule

1. *Connection between the generalized densities and a higher elastic Green's function*

We start from the six-point, three-times Green's function

$$\begin{aligned} R_{pqrstu}(t,t',t'') \;=\; & - < 0|\hat{T}\left[c_p^\dagger(t)c_q(t)c_r^\dagger(t')c_s(t')c_t^\dagger(t'')c_u(t'')\right]|0> \\ & + < 0|\hat{T}\left[c_p^\dagger(t)c_q(t)c_r^\dagger(t')c_s(t')\right]|0>< 0|c_t^\dagger(t'')c_u(t'')|0> \\ & + < 0|\hat{T}\left[c_p^\dagger(t)c_q(t)c_t^\dagger(t'')c_u(t'')\right]|0>< 0|c_r^\dagger(t')c_s(t')|0> \\ & + < 0|\hat{T}\left[c_r^\dagger(t')c_s(t')c_t^\dagger(t'')c_u(t'')\right]|0>< 0|c_p^\dagger(t)c_q(t)|0> \\ & -2 < 0|c_p^\dagger(t)c_q(t)|0>< 0|c_r^\dagger(t')c_s(t')|0>< 0|c_t^\dagger(t'')c_u(t'')|0>, \end{aligned} \tag{66}$$

which is very similar to the one used in the direct approach (compare section II B). Essentially, it can be obtained from the latter one by setting the two central time arguments equal

and interchanging the corresponding annihilation and creation operators. Also here, the extra factors which are subtracted and added to the six-operator expectation value eliminate the disjoint diagrams in the diagrammatic expansion, and the overall sign is chosen to give a convenient spectral representation.

Due to the reduced number of time arguments, we have here only six different possible time orderings. All six contributions depend only on the two time differences $\tau = t - t'$ and $\tau' = t' - t''$, and hence we can write:

$$\begin{aligned} R_{pqrstu}(t,t',t'') \;=\; & \theta(\tau)\theta(\tau')R^{(I)}_{pqrstu}(\tau,\tau') + \theta(\tau+\tau')\theta(-\tau')R^{(II)}_{pqrstu}(\tau,\tau') \\ & +\theta(-\tau)\theta(\tau+\tau')R^{(III)}_{pqrstu}(\tau,\tau') + \theta(-\tau-\tau')\theta(\tau')R^{(IV)}_{pqrstu}(\tau,\tau') \\ & +\theta(\tau)\theta(-\tau-\tau')R^{(V)}_{pqrstu}(\tau,\tau') + \theta(-\tau)\theta(-\tau')R^{(VI)}_{pqrstu}(\tau,\tau'). \end{aligned}$$

Performing the same mathematical steps as in the preceding sections, we arrive at

$$\begin{aligned} R^{(I)}_{pqrstu}(\tau,\tau') \;=\; & -\sum_{M\neq 0, N\neq 0} \rho^{[0,M]}_{pq}\rho^{[N,0]}_{tu}\left(\rho^{[M,N]}_{rs} - \delta_{MN}\rho^{[0,0]}_{rs}\right) \\ & \cdot e^{-i(E^{[M]}-E^{[0]})\tau} e^{-i(E^{[N]}-E^{[0]})\tau'}. \end{aligned}$$

Fourier transforming with respect to both time differences yields

$$R^{(I)}_{pqrstu}(\omega,\omega') \;=\; +\sum_{M\neq 0, N\neq 0} \frac{\rho^{[0,M]}_{pq}\left(\rho^{[M,N]}_{rs} - \delta_{MN}\rho^{[0,0]}_{rs}\right)\rho^{[N,0]}_{tu}}{(\omega - (E^{[M]}-E^{[0]}) + i0^+)(\omega' - (E^{[N]}-E^{[0]}) + i0^+)}. \quad (67)$$

The poles of the Green's function (in both variables) are given by the energy differences between the excited states and the ground state, and the residues of the double poles yield the generalized one-particle densities. Analogously to the direct approach, the knowledge of the one-particle density of the ground state is not necessary if one modifies the definition of R by subtracting less terms, like in eq.(9). Then, one can obtain the spectral decomposition

$$R^{(I)}_{pqrstu}(\omega,\omega') = \sum_{M\neq 0, N\neq 0} \frac{\rho^{[0,M]}_{pq}}{\omega - (E^{[M]}-E^{[0]}) + i0^+}\rho^{[M,N]}_{rs}\frac{\rho^{[N,0]}_{tu}}{\omega' - (E^{[N]}-E^{[0]}) + i0^+}. \quad (68)$$

Although this approach is appealing, one would have to include a large number of disjoint diagrams in the computation.

Using the same mathematical steps on the other five components of R, correspondings to the other five time orderings, it turns out that they are related to $R^{(1)}$ in a simple way:

$$R^{(II)}_{pqrstu}(\omega,\omega') \;=\; R^{(I)}_{pqturs}(\omega,\omega-\omega')$$

$$
\begin{aligned}
R^{(III)}_{pqrstu}(\omega,\omega') &= R^{(I)}_{rspqtu}(\omega'-\omega,\omega') \\
R^{(IV)}_{pqrstu}(\omega,\omega') &= R^{(I)}_{rstupq}(\omega'-\omega,-\omega) \\
R^{(V)}_{pqrstu}(\omega,\omega') &= R^{(I)}_{tupqrs}(-\omega',\omega-\omega') \\
R^{(VI)}_{pqrstu}(\omega,\omega') &= R^{(I)}_{turspq}(-\omega',-\omega).
\end{aligned}
$$

Clearly, it is sufficient to calculate $R^{(I)}$—the other five components contain the same physical information.

2. Diagrammatic representation

The higher elastic Green's function can be calculated with the help of Feynman diagrams and rules. The rules here are almost identical to the ones presented in section II B. The main difference lies in rule (F1): we have now at all three times t, t' and t'' both a line starting and a line ending there. Rule (G3) simplifies, since we have only two time differences now instead of the three before:

(G3) We introduce two auxiliary lines, going from t to t' and from t' to t''. Each cut between two successive vertices (including the external) introduces a denominator of the type

$$\sigma\omega + \sigma'\omega' + \epsilon_k + \epsilon_l + \ldots - \epsilon_i - \epsilon_j - \ldots + i0^+.$$

The energy variables ω, ω' are introduced if the first or second auxiliary line is cut, respectively, and have positive ($\sigma = +1$ or $\sigma' = +1$, respectively) or negative signs ($\sigma = -1$ or $\sigma' = -1$, respectively) according to the downward or upward direction of the corresponding auxiliary line. If none of the auxiliary lines is cut, then $\sigma = \sigma' = 0$, and a constant denominator results in which the imaginary infinitesimal $i0^+$ can be omitted.

Other rules presented in section II B also change slightly. The overall factor for the Feynman diagrams in rule (F4) is now $(-1)(-i)^n i^{2n+3} = i^{n+1}$, the overall factor for the Goldstone diagrams in rule (G4) is $(-1)(-i)^n i^{n+2} = +1$. The rule for the additional sign factor is now simply: multiply with -1 if only equal times are connected (i. e. t to t, t' to t', and t'' to t'') or if only unequal times are connected; multiply with $+1$ otherwise.

The $(n+3)!$ Goldstone diagrams can be divided into six classes of diagrams according to the six possible time orderings of t, t' and t'' for the external vertices. The diagrams of a given time ordering contribute only to the respective parts of R.

The number of Feynman diagrams in order n is here the same as in the direct approach (see section II B), and the diagrams look very similar. Actually, the Goldstone diagrams can be obtained from the diagrams of the direct approach by dropping all diagrams which have an interaction vertex between the dotted lines corresponding to the times t and t', and letting these two dotted lines merge into one line for the remaining diagrams.

For a given time ordering of the external vertices in order n, one here only has to consider $(n+3)!/3!$ (=1, 4, 20, ...) different Goldstone diagrams for every Feynman diagram. Hence the number of Goldstone diagrams for a given time ordering of the external vertices in order n is considerably lower than in the direct approach:

- $n = 0$: 2 (Fig. 15)
- $n = 1$: 24 (Fig. 16)
- $n = 2$: 720

The 36 Feynman diagrams of the second order are shown in Fig. 17.

Since we have here only three instead of four time arguments, there is a reduction in the number of Goldstone diagrams by a factor of $4/(n+4)$ compared to the direct approach. Additionally, one has to consider that we now have to evaluate only the diagrams for one time ordering of the external vertices. This yields the generalized densities, and from these one can then obtain the particle and the hole component of the natural, the scattering-motivated or the ionization-motivated Green's function—all from this one single result. In contrast, different time orderings of the external vertices have to be considered in the direct approach.

One can obtain the generalized densities by evaluating the diagrams with a method similar to the one used in the direct approach (section II B). The results are:

$$\begin{aligned}
\rho_{rs}^{[\bar{p}q,t\bar{u}](0,1)} &= \bar{n}_r\bar{n}_s\delta_{pu}\delta_{qr}\delta_{st} - n_r n_s\delta_{ps}\delta_{qt}\delta_{ru} + (\bar{n}_r n_s - n_r\bar{n}_s)(\delta_{pu}v_{sqrt} - \delta_{qt}v_{surp}) \\
&\quad +\bar{n}_s\delta_{st}v_{qupr}(1-\delta_{pu}\delta_{qr}) - n_r\delta_{ru}v_{qspt}(1-\delta_{ps}\delta_{qt}) \\
&\quad -\bar{n}_r\delta_{qr}v_{ustp}(1-\delta_{pu}\delta_{st}) + n_s\delta_{ps}v_{uqtr}(1-\delta_{qt}\delta_{ru}) \qquad (69) \\
\rho_{rs}^{[\bar{p}q,a\bar{b}c\bar{d}](0)} &= (\delta_{aq}\delta_{cs} - \delta_{as}\delta_{cq})(\delta_{bp}\delta_{dr} - \delta_{br}\delta_{dp}) \qquad (70) \\
\rho_{rs}^{[a\bar{b}c\bar{d},t\bar{u}](0)} &= (\delta_{ar}\delta_{ct} - \delta_{at}\delta_{cr})(\delta_{bs}\delta_{du} - \delta_{bu}\delta_{ds}), \qquad (71)
\end{aligned}$$

FIG. 15: Goldstone diagrams for the first component $R^{(I)}$ of the three-times Green's function for a closed-shell molecule in zeroth order

where the superscript $(0,1)$ means the contributions of both zeroth and first order. When determining the latter two densities, it is helpful to have the generalized densities $T^{[2]}$ already available. Note that using the same matrix notation as in section II B, the polarization propagator can be written as

$$\Pi^{+}_{pqrs}(\omega) = \mathbf{T}^{\dagger}_{qp}\frac{1}{\omega - \mathbf{E} - \mathbf{V}}\mathbf{T}_{rs}.$$

Thus the $T^{[2]}$ can be obtained from the literature on the polarization propagator (e. g. [27]).

We will demonstrate in the next section how to derive the inelastic propagator from the generalized densities explicitly in first order. This is exemplarily carried out for the closed-shell anion case, since there the number of terms one has to consider is considerably lower, and thus the calculation is more transparent.

C. Closed-shell anion

1. *Connection between the generalized densities and a higher elastic Green's function*

Here we make use of the following four-point, three-times Green's function

$$\begin{aligned} R_{pqrs}(t,t',t'') \;=\; & - < 0^{-}|\hat{T}\left[c^{\dagger}_{p}(t)c^{\dagger}_{q}(t')c_{r}(t')c_{s}(t'')\right]|0^{-}> \\ & + < 0^{-}|\hat{T}\left[c^{\dagger}_{p}(t)c_{s}(t'')\right]|0^{-}>< 0^{-}|c^{\dagger}_{q}(t')c_{r}(t')|0^{-}> . \end{aligned} \tag{72}$$

The notation is the same as in section II C. As in the case of a closed-shell neutral molecule, this Green's function can be obtained from the one used in the direct approach by setting the two central time arguments equal and interchanging the corresponding annihilation and creation operators.

Again, there are six different time orderings possible here. All depend only on the two time differences $\tau = t - t'$ and $\tau' = t' - t''$, and we can write the Green's function as a sum of six terms, just as we have done in the case of a closed-shell molecule in section III B.

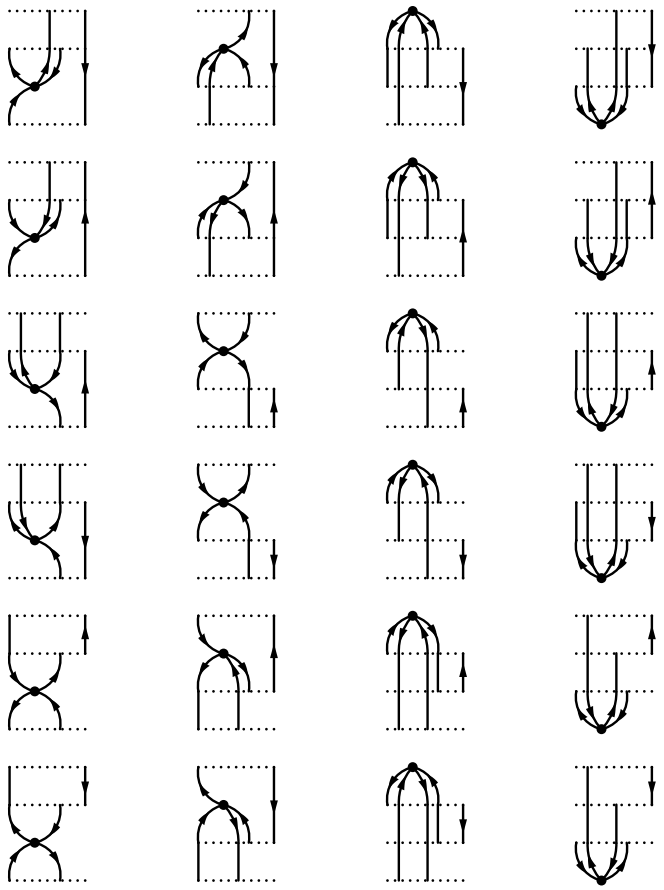

FIG. 16: Goldstone diagrams for the first component $R^{(I)}$ of the three-times Green's function for a closed-shell molecule in first order

By inserting complete sets of energy eigenstates $|N>$ of the neutral open-shell molecule, we obtain

$$R^{(I)}_{pqrs}(\omega,\omega') \;=\; +\sum_{M,N} \frac{x_p^{[M]\dagger}\left(\rho_{qr}^{[M,N]} - \delta_{MN}\rho_{qr}^{[0^-,0^-]}\right) x_s^{[N]}}{(\omega - (E^{[M]} - E^{[0^-]}) + i0^+)(\omega' - (E^{[N]} - E^{[0^-]}) + i0^+)}. \qquad (73)$$

In other words, one obtains the generalized one-particle density of the neutral open-shell system from the residues of the Green's function R defined in (72) for the closed-shell anion.

Using the same mathematical steps on the other five components of R, which correspond to the other five time orderings, it turns out that they provide *different* physical information than $R^{(I)}$, but that information (e. g. transition amplitudes from the anion to the dianion, and dianion energies) is not of interest here.

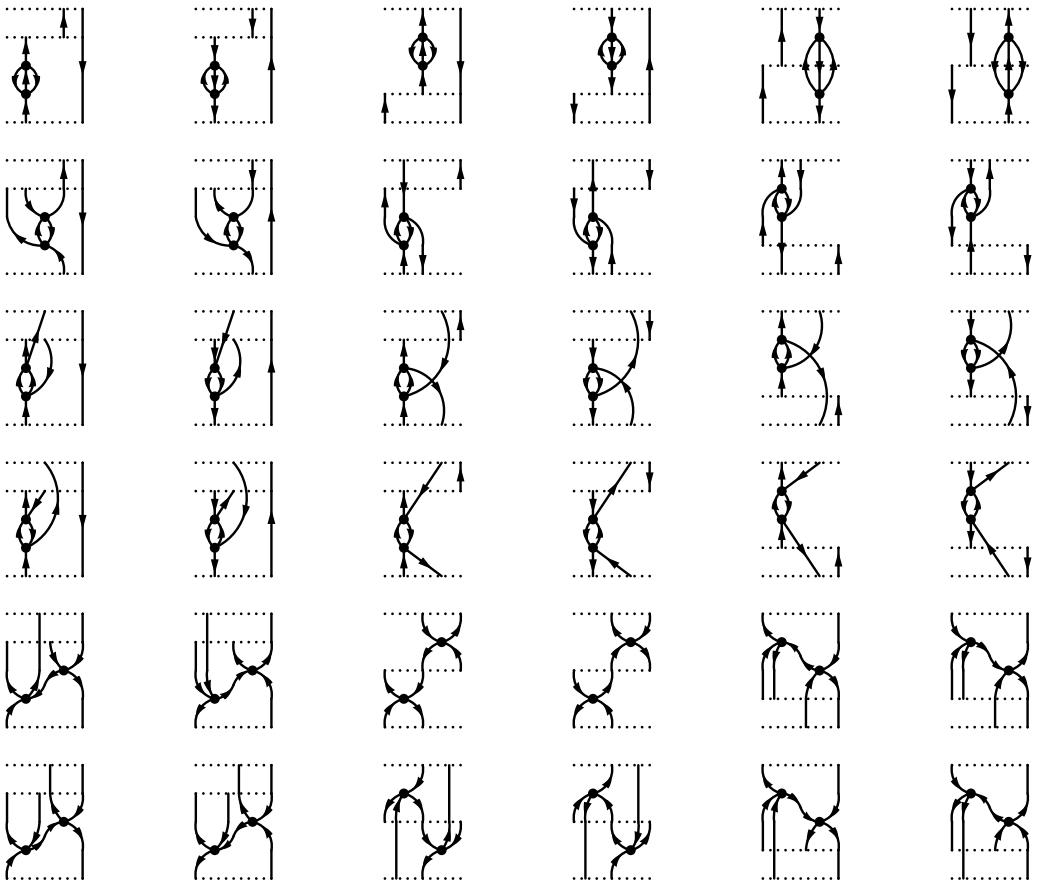

FIG. 17: Feynman diagrams for the three-times Green's function for a closed-shell molecule in second order

2. Diagrammatic representation

The Feynman rules are almost identical to the ones used in the direct approach (see section II B). In rule (F1), we have now one line starting at time t' and one at t, and one line ending at time t' and one at time t''. Rule (G3) is the same as in the Dyson approach to the closed-shell neutral molecule (see section III B). The overall factor for the Feynman diagrams in rule (F4) is now $(-1)(-i)^n i^{2n+2} = i^n$, the overall factor for the Goldstone diagrams in rule (G4) is $(-1)(-i)^n i^{n+2} = +1$. The additional sign factor is here $+1$ if t' is connected to itself, and -1 otherwise.

The $(n+3)!$ Goldstone diagrams can be divided into six sets of diagrams according to the six possible time orderings of t, t' and t'' for the external vertices. Each set of diagrams

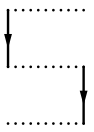

FIG. 18: Goldstone diagrams for the first component $R^{(I)}$ of the three-times Green's function for a closed-shell anion in zeroth order

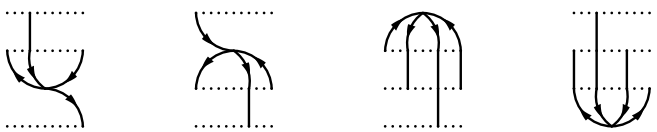

FIG. 19: Goldstone diagrams for the first component $R^{(I)}$ of the three-times Green's function for a closed-shell anion in first order

contributes only to the respective component of R.

The number of Feynman diagrams in order n is the same as in the direct approach. But since we have to consider only $(n+3)!/3!$ different Goldstone diagrams for every Feynman diagram and a given time ordering of the external vertices, the number of Goldstone diagrams one has to evaluate in order n is now relatively moderate:

- $n = 0$: 1 (Fig. 18)
- $n = 1$: 4 (Fig. 19)
- $n = 2$: 100

The five Feynman diagrams in the second order are shown in Fig. 20.

The usage of only three instead of the four different times in the direct approach leads to a reduction in the number of Goldstone diagrams by a factor of $4/(n+4)$, although the number of Feynman diagrams stays the same. One could even consider the third order, where one has 23 Feynman diagrams. These look very similar to the Feynman diagrams for the polarization propagator in third order [30]. There are 120 Goldstone diagrams for every Feynman diagram, and hence 2760 Goldstone diagrams to evaluate. This is a quite demanding task, but still in a feasible range.

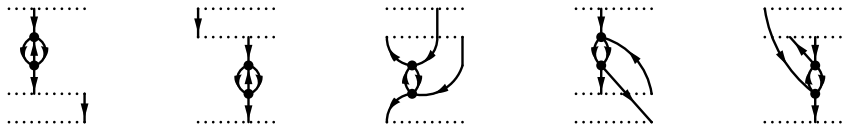

FIG. 20: Feynman diagrams for the three-times Green's function for a closed-shell anion in second order

3. Calculating the particle component of the inelastic Green's function with the Dyson-like equation

The explicit results for the four diagrams in first order are given in appendix 3. Evaluating them with methods very similar to the ones used in the direct approach (compare section II C), we obtain the generalized densities:

$$\rho_{qr}^{[\bar{p},\bar{s}](0,1)} = n_r\delta_{ps}\delta_{qr} - \delta_{pr}\delta_{sq} + v_{rspq}\left(\bar{n}_q n_r - n_q\bar{n}_r\right) \tag{74}$$

$$\rho_{qr}^{[\bar{p},\bar{s}\bar{t}u](0)} = \delta_{ru}\left(\delta_{ps}\delta_{qt} - \delta_{pt}\delta_{qs}\right) \tag{75}$$

$$\rho_{qr}^{[\bar{s}\bar{t}u,\bar{p}](0)} = \delta_{qu}\left(\delta_{ps}\delta_{rt} - \delta_{pt}\delta_{rs}\right). \tag{76}$$

Just as in the direct approach, it turns out that the energies of the excited states receive no contribution in first order. This implies that $\tilde{G}$ also receives no contribution in first order [see eq.(62)], and hence

$$\tilde{G}_{qr}^{[\bar{p},\bar{s}](0,1)}(\omega) = \frac{\delta_{qr}\delta_{ps}n_p n_s}{\omega - (\epsilon_p - \epsilon_q) + i0^+} + 0. \tag{77}$$

Additionally, we have

$$\tilde{G}_{qr}^{[\bar{p},\bar{s}\bar{t}u](0,1)}(\omega) = \tilde{G}_{qr}^{[\bar{s}\bar{t}u,\bar{p}](0,1)}(\omega) = 0 \tag{78}$$

and

$$\tilde{G}_{pq}^{[\bar{a}\bar{b}c,\bar{d}\bar{e}f](0)}(\omega) = \frac{\delta_{pq}n_a n_b\bar{n}_c n_d n_e\bar{n}_f\delta_{ct}\left(\delta_{ad}\delta_{be} - \delta_{ae}\delta_{bd}\right)}{\omega - (\epsilon_p - \epsilon_a - \epsilon_b + \epsilon_c) + i0^+}. \tag{79}$$

Using eq.(65), we can also easily determine

$$\rho_{qr}^{+[\bar{p},\bar{s}](0,1)} = \bar{n}_r\delta_{ps}\delta_{qr} + \delta_{pq}\delta_{rs} + v_{qspr}\left(\bar{n}_q n_r - n_q\bar{n}_r\right) \tag{80}$$

$$\rho_{qr}^{+[\bar{p},\bar{s}\bar{t}u](0)} = \delta_{qu}\left(\delta_{ps}\delta_{rs} - \delta_{pt}\delta_{rt}\right) \tag{81}$$

$$\rho_{qr}^{+[\bar{s}\bar{t}u,\bar{p}](0)} = \delta_{ru}\left(\delta_{pt}\delta_{qs} - \delta_{ps}\delta_{qt}\right). \tag{82}$$

Employing again a matrix notation like in section II C, with the subblocks denoted by 1,2, etc. in square brackets, we can then write the Dyson equation for the particle component of

the natural inelastic propagator up to first order in the following form:

$$\begin{aligned}\mathbf{G}^{+[1,1](1)} &= \tilde{\mathbf{G}}^{[1,1](0)}\boldsymbol{\rho}^{+[1,1](1)} + \tilde{\mathbf{G}}^{[1,1](0)}\mathbf{A}^{+[1,1](1)}\tilde{\mathbf{G}}^{[1,1](0)}\boldsymbol{\rho}^{+[1,1](0)} \\ &\quad + \tilde{\mathbf{G}}^{[1,1](0)}\mathbf{A}^{+[1,2](1)}\tilde{\mathbf{G}}^{[2,2](0)}\boldsymbol{\rho}^{+[2,1](0)}, \end{aligned} \tag{83}$$

plus several other terms which vanish due to the vanishing components of $\tilde{\mathbf{G}}$ given above.

Using the definition (58) of $\mathbf{A}^+$, inserting the Hartree-Fock one-particle interaction

$$W_{pq} = -\sum_n V_{pn[qn]} n_n$$

and the results given about, we arrive at

$$\begin{aligned}\tilde{\mathbf{G}}^{[1,1](0)}\boldsymbol{\rho}^{+[1,1](1)} &= \frac{V_{qs[pr]}\left(\bar{n}_q n_r - n_q \bar{n}_r\right)}{(\epsilon_q + \epsilon_s - \epsilon_p - \epsilon_r)(\omega - \epsilon_q + \epsilon_p + i0^+)} \\ \tilde{\mathbf{G}}^{[1,1](0)}\mathbf{A}^{+[1,1](1)}\tilde{\mathbf{G}}^{[1,1](0)}\boldsymbol{\rho}^{+[1,1](0)} &= \frac{1}{2}\bar{n}_r \frac{V_{qs[pr]} - \sum_n V_{qn[rn]} n_n \delta_{ps}}{(\omega - \epsilon_q + \epsilon_p + i0^+)(\omega - \epsilon_r + \epsilon_s + i0^+)} \\ \tilde{\mathbf{G}}^{[1,1](0)}\mathbf{A}^{+[1,2](1)}\tilde{\mathbf{G}}^{[2,2](0)}\boldsymbol{\rho}^{+[2,1](0)} &= \frac{1}{2}\bar{n}_r \frac{V_{qs[pr]} + \sum_n V_{qn[rn]} n_n \delta_{ps}}{(\omega - \epsilon_q + \epsilon_p + i0^+)(\omega - \epsilon_r + \epsilon_s + i0^+)}\end{aligned}$$

Adding everything together, the terms with

$$\sum_n V_{qn[rn]} n_n,$$

which correspond to "tadpole" graphs, cancel out, and we finally obtain

$$G_{qr}^{+n[\bar{p},\bar{s}](1)} = \frac{V_{qs[pr]}}{\epsilon_q + \epsilon_s - \epsilon_p - \epsilon_r}\left[\frac{\bar{n}_q}{\omega - (\epsilon_q - \epsilon_p) + i0^+} - \frac{\bar{n}_r}{\omega - (\epsilon_r - \epsilon_s) + i0^+}\right], \tag{84}$$

which agrees completely with the result (48) from the direct approach.

We see here that even after one has obtained the generalized densities from the diagrams, one still needs to carry out some additional manipulations until one actually obtains the desired inelastic Green's function. Furthermore, in order to get the inelastic propagator for one particular type of excited states (here: $1h$ states), it is not sufficient to take the corresponding generalized densities into account—one also needs the generalized densities for other states (here: $2h1p$ states).

Therefore, even if one wants to obtain only $\mathbf{G}^{[1,1](n)}$, one has to consider *all* $(n+3)!/3!$ time orderings of the Feynman diagrams. In contrast, only $(n+2)!/2!$ time orderings were needed for this special case in the direct approach. On the other hand, if one desires also the propagators between higher excited states, one would have to take into account $(n+4)!/4!$ time orderings in the direct approach, but only $(n+3)!/3!$ time orderings in the Dyson approach presented here.

D. Closed-shell cation

1. Connection between the generalized densities and a higher elastic Green's function

This case is very similar to that of a closed-shell anion, and we may present the results briefly. We now use the following four-point, three-times Green's function

$$\begin{aligned} R_{pqrs}(t,t',t'') \;=\; & - < 0^+|\hat{T}\left[c_p(t)c_q^\dagger(t')c_r(t')c_s^\dagger(t'')\right]|0^+> \\ & + < 0^+|\hat{T}\left[c_p(t)c_s^\dagger(t'')\right]|0^+>< 0^+|c_q^\dagger(t')c_r(t')|0^+>, \end{aligned} \tag{85}$$

where $|0^+>$ denotes the ground state of the (closed-shell) cation of the open-shell target.

By inserting complete sets of energy eigenstates $|N>$ of the neutral open-shell molecule, we obtain here

$$\begin{aligned} R^{(I)}_{pqrs}(\omega,\omega') \;=\; & + \sum_{M,N} \frac{y_p^{[M]\dagger}}{\omega - (E^{[M]} - E^{[0^+]}) + i0^+} \frac{y_s^{[N]}}{\omega' - (E^{[N]} - E^{[0^+]}) + i0^+} \\ & \cdot \left(\rho_{qr}^{[M,N]} - \delta_{MN}\rho_{qr}^{[0^+,0^+]}\right). \end{aligned} \tag{86}$$

Again, the generalized one-particle density can be obtained from the residues of this Greens' function.

Just as in the case of the closed-shell anion, the other five time orderings $R^{(II)}$ to $R^{(VI)}$ provide *different* physical information—but this information is not of interest in the present context (e. g. transition amplitudes from the cation to the dication).

2. Diagrammatic representation

The Feynman rules are almost the same as in the closed-shell anion case (compare section III C). The main difference is that we have now a line starting at time t' and a line ending at time t. The additional sign factor in the rules (F4) and (G4) is also different: it is here -1 if t' is connected to itself and $+1$ otherwise. The Feynman diagrams look very similar—the only difference lies in the direction of the external lines. The Goldstone diagrams in zeroth and first order are shown in Figs. 21 and 22, and the Feynman diagrams of second order are shown in Fig. 23.

Evaluating the single diagram in zeroth and the four diagrams in first order, we obtain the following generalized densities:

$$\rho_{qr}^{[p,s](0,1)} \;=\; n_r\delta_{ps}\delta_{qr} + \delta_{pq}\delta_{rs} + v_{rpqs}\left(\bar{n}_q n_r - n_q\bar{n}_r\right) \tag{87}$$

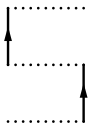

FIG. 21: Goldstone diagrams for the first component $R^{(I)}$ of the three-times Green's function for a closed-shell cation in zeroth order

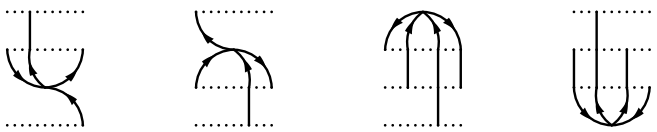

FIG. 22: Goldstone diagrams for the first component $R^{(I)}$ of the three-times Green's function for a closed-shell cation in first order

$$\rho_{qr}^{[p,st\bar{u}](0)} = \delta_{qu}\left(\delta_{ps}\delta_{rt} - \delta_{pt}\delta_{rs}\right) \tag{88}$$

$$\rho_{qr}^{[st\bar{u},p](0)} = \delta_{ru}\left(\delta_{ps}\delta_{qt} - \delta_{pt}\delta_{qs}\right). \tag{89}$$

The inelastic Green's functions can then be obtained in analogy to those obtained in section III C.

IV. DISCUSSION AND CONCLUSIONS

Two different methods, the *direct approach* and the *Dyson approach*, for determining the inelastic propagator were presented in this work. Both can be used to obtain the natural, the scattering-motivated and the ionization-motivated inelastic Green's function. Furthermore, both are applicable for closed- and also for open-shell molecules, provided that there exists a closed-shell anion or cation. An extension of the method to cases where both the neutral molecule and the singly charged molecules are open-shell, but the dianion or dication is

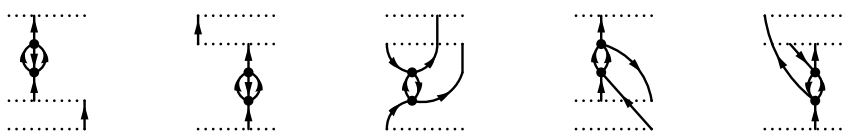

FIG. 23: Feynman diagrams for the three-times Green's function for a closed-shell cation in second order

closed-shell, would be rather straightforward. The resulting diagrams would be similar to those in the closed-shell neutral molecule case.

The direct approach yields the inelastic propagator itself by evaluating the diagrams for the elastic six-point, four-times Green's function. From the point of view of this construction scheme, the scattering- and the ionization-motivated Green's function look in a way more "natural" than the natural Green's function—they can be both obtained consistently from the single formulas (14) and (15), respectively, whereas the two different formulas (16) and (17) have to be combined in order to get the natural Green's function. But in the actual diagrammatic evaluation, it turned out that the natural Green's function is easier to obtain after all—it is not plagued by additional, spurious phase factors.

A drawback of the direct approach is that even in low orders the necessary number of diagrams is already quite large (especially for closed-shell neutral molecules). Nevertheless, we think that the formalism provides promising opportunities for theoretical studies of the inelastic propagator. For example, it should be possible to obtain diagrammatic rules for the inelastic self-energy, which is an optical potential for inelastic scattering [21]. In addition, it has to be noted that a significant reduction in the number of diagrams can be achieved in those relevant cases where propagators only between singly excited states are desired. In that case, the direct approach should be of good practical use. In contrast, if all inelastic propagators are of interest, the Dyson approach is preferable, since it requires a significantly lower number of diagrams.

Csanak and coworkers have presented methods similar to our direct approach [see especially eq. (9) in [15]] and also equations involving higher order Green's functions. With these methods, they calculated Bethe-Salpeter amplitudes, which differ from our Green's functions by phase factors. They also gave an interpretation of their formulas with Feynman-type diagrams. But in contrast to our approach, they did not develop a systematic diagrammatic approach employing the evaluation of higher order Green's functions with Feynman rules. Further advantages are that our formalism is also applicable to molecules which only possess a closed-shell ion, and can provide all three types of inelastic Green's functions directly instead of only the Bethe-Salpeter amplitudes.

An obvious generalization of our straightforward diagrammatic expansion would be to combine the successful Algebraic Diagrammatic Construction scheme [1, 27, 30] with the direct approach, in order to be able to include systematically higher order corrections to the

inelastic propagator. Therefore, it would be desirable to have a method to evaluate directly the diagrams of the inelastic propagator instead of those of the higher multi-times Green's function, from which one has to extract the desired inelastic propagator. We currently work on the development of such a method.

As already pointed out, the approach using the Dyson-like equations and generalized density provides the inelastic propagators by evaluating significantly less diagrams than the direct approach. Interestingly, the Dyson-like equations can also provide further insights into the underlying physics.

It should be remarked here that if the projectile is distinguishable from the particles of the target, A^+ [see eq.(58)] provides already an optical potential for the scattering [18, 21]. In this case, calculating the generalized densities is already sufficient for solving the scattering problem, and the inelastic propagator itself is not explicitly needed. Here, the Dyson approach is obviously much more appropriate than the direct approach.

On the other hand, if the projectile is indistinguishable from the target's particles, the full inelastic propagator is needed. To obtain it from the generalized densities, a considerable amount of additional work is required. Furthermore, it is a rather inconvenient fact that generalized densities for higher excited states are necessary for calculating the propagator between low excited states. It is also unclear yet how one can obtain a diagrammatic representation of the inelastic self-energy by using this approach.

A possible alternative method for obtaining the generalized densities was recently developed by Schirmer and Trofimov [31] with the help of the Algebraic Diagrammatic Construction scheme mentioned above. But we think that our diagrammatic approach is more transparent and can thus serve better for a systematic treatment and interpretation of the various contributions.

Summarizing, the methods presented here provide systematic diagrammatic approximation schemes for the various inelastic propagators. For the cases of the closed-shell anion and cation, the second order approximation is easily feasible, and even the third order should be viable. The methods should also be well suited for theoretical investigations of the inelastic propagator and for obtaining a better understanding of the underlying physics. Combinations with already known approximation methods like the Algebraic Diagrammatic Construction scheme should be possible to obtain.

Acknowledgments

We thank J. Schirmer for help with the theory and the drawing of Feynman diagrams.

APPENDIX: CONTRIBUTIONS IN FIRST ORDER

1. Four-times Green's function for a closed-shell neutral molecule

The contributions of the 30 diagrams shown in Fig. 4 are listed below.

$$
\begin{aligned}
1a &= -n_p\bar{n}_q\bar{n}_r\bar{n}_s\bar{n}_t n_u\delta_{pu}V_{qr[st]}\frac{1}{\omega_f+\epsilon_p-\epsilon_q+i0^+}\frac{1}{\omega+\epsilon_p-\epsilon_q-\epsilon_r+i0^+}\\
&\cdot\frac{1}{\omega-\epsilon_s-\epsilon_t+\epsilon_u+i0^+}\frac{1}{\omega_i-\epsilon_t+\epsilon_u+i0^+}\\
1b &= n_p\bar{n}_q\bar{n}_r n_s\bar{n}_t n_u\delta_{pu}V_{qr[st]}\frac{1}{\omega_f+\epsilon_p-\epsilon_q+i0^+}\frac{1}{\omega+\epsilon_p-\epsilon_q-\epsilon_r+i0^+}\\
&\cdot\frac{1}{\omega_i+\epsilon_p-\epsilon_q-\epsilon_r+\epsilon_s+i0^+}\frac{1}{\omega_i-\epsilon_t+\epsilon_u+i0^+}\\
1c &= n_p\bar{n}_q n_r\bar{n}_s\bar{n}_t n_u\delta_{pu}V_{qr[st]}\frac{1}{\omega_f+\epsilon_p-\epsilon_q+i0^+}\frac{1}{\omega_f+\epsilon_r-\epsilon_s-\epsilon_t+\epsilon_u+i0^+}\\
&\cdot\frac{1}{\omega-\epsilon_s-\epsilon_t+\epsilon_u+i0^+}\frac{1}{\omega_i-\epsilon_t+\epsilon_u+i0^+}\\
1d &= -n_p n_q n_r\bar{n}_s\bar{n}_t n_u\delta_{pu}V_{qr[st]}\frac{1}{\epsilon_q+\epsilon_r-\epsilon_s-\epsilon_t}\frac{1}{\omega_f+\epsilon_p+\epsilon_r-\epsilon_s-\epsilon_t+i0^+}\\
&\cdot\frac{1}{\omega-\epsilon_s-\epsilon_t+\epsilon_u+i0^+}\frac{1}{\omega_i-\epsilon_t+\epsilon_u+i0^+}\\
1e &= -n_p\bar{n}_q\bar{n}_r n_s n_t n_u\delta_{pu}V_{qr[st]}\frac{1}{\omega_f+\epsilon_p-\epsilon_q+i0^+}\frac{1}{\omega+\epsilon_p-\epsilon_q-\epsilon_r+i0^+}\\
&\cdot\frac{1}{\omega_i+\epsilon_p-\epsilon_q-\epsilon_r+\epsilon_s+i0^+}\frac{1}{-\epsilon_q-\epsilon_r+\epsilon_s+\epsilon_t}\\
2a &= n_p\bar{n}_q\bar{n}_r\bar{n}_s\bar{n}_t n_u\delta_{qt}V_{ru[ps]}\frac{1}{\omega_f+\epsilon_p-\epsilon_q+i0^+}\frac{1}{\omega+\epsilon_p-\epsilon_q-\epsilon_r+i0^+}\\
&\cdot\frac{1}{\omega-\epsilon_s-\epsilon_t+\epsilon_u+i0^+}\frac{1}{\omega_i-\epsilon_t+\epsilon_u+i0^+}\\
2b &= -n_p\bar{n}_q\bar{n}_r n_s\bar{n}_t n_u\delta_{qt}V_{ru[ps]}\frac{1}{\omega_f+\epsilon_p-\epsilon_q+i0^+}\frac{1}{\omega+\epsilon_p-\epsilon_q-\epsilon_r+i0^+}\\
&\cdot\frac{1}{\omega_i+\epsilon_p-\epsilon_q-\epsilon_r+\epsilon_s+i0^+}\frac{1}{\omega_i-\epsilon_t+\epsilon_u+i0^+}\\
2c &= -n_p\bar{n}_q n_r\bar{n}_s\bar{n}_t n_u\delta_{qt}V_{ru[ps]}\frac{1}{\omega_f+\epsilon_p-\epsilon_q+i0^+}\frac{1}{\omega_f+\epsilon_r-\epsilon_s-\epsilon_t+\epsilon_u+i0^+}\\
&\cdot\frac{1}{\omega-\epsilon_s-\epsilon_t+\epsilon_u+i0^+}\frac{1}{\omega_i-\epsilon_t+\epsilon_u+i0^+}
\end{aligned}
$$

$$
\begin{aligned}
2d &= \bar{n}_p\bar{n}_q n_r\bar{n}_s\bar{n}_t n_u\delta_{qt}V_{ru[ps]}\frac{1}{\epsilon_r+\epsilon_u-\epsilon_p-\epsilon_s}\frac{1}{\omega_f-\epsilon_q+\epsilon_r-\epsilon_s+\epsilon_u+i0^+}\\
&\cdot\frac{1}{\omega-\epsilon_q-\epsilon_s+\epsilon_u+i0^+}\frac{1}{\omega_i-\epsilon_t+\epsilon_u+i0^+}\\
2e &= n_p\bar{n}_q\bar{n}_r n_s\bar{n}_t\bar{n}_u\delta_{qt}V_{ru[ps]}\frac{1}{\omega_f+\epsilon_p-\epsilon_q+i0^+}\frac{1}{\omega+\epsilon_p-\epsilon_q-\epsilon_r+i0^+}\\
&\cdot\frac{1}{\omega_i+\epsilon_p-\epsilon_q-\epsilon_r+\epsilon_s+i0^+}\frac{1}{-\epsilon_r-\epsilon_u+\epsilon_p+\epsilon_s}\\
3a &= n_p\bar{n}_q\bar{n}_r\bar{n}_s\bar{n}_t n_u\delta_{rt}V_{uq[ps]}\frac{1}{\omega_f+\epsilon_p-\epsilon_q+i0^+}\frac{1}{\omega+\epsilon_p-\epsilon_q-\epsilon_r+i0^+}\\
&\cdot\frac{1}{\omega-\epsilon_s-\epsilon_t+\epsilon_u+i0^+}\frac{1}{\omega_i-\epsilon_t+\epsilon_u+i0^+}\\
3b &= -n_p\bar{n}_q\bar{n}_r n_s\bar{n}_t n_u\delta_{rt}V_{uq[ps]}\frac{1}{\omega_f+\epsilon_p-\epsilon_q+i0^+}\frac{1}{\omega+\epsilon_p-\epsilon_q-\epsilon_r+i0^+}\\
&\cdot\frac{1}{\omega_i+\epsilon_p-\epsilon_q-\epsilon_r+\epsilon_s+i0^+}\frac{1}{\omega_i-\epsilon_t+\epsilon_u+i0^+}\\
3c &= n_p\bar{n}_q\bar{n}_r\bar{n}_s\bar{n}_t n_u\delta_{rt}V_{uq[ps]}\frac{1}{\omega_f+\epsilon_p-\epsilon_q+i0^+}\frac{1}{\omega_f-\epsilon_s+\epsilon_u+i0^+}\\
&\cdot\frac{1}{\omega-\epsilon_s-\epsilon_t+\epsilon_u+i0^+}\frac{1}{\omega_i-\epsilon_t+\epsilon_u+i0^+}\\
3d &= \bar{n}_p n_q\bar{n}_r\bar{n}_s\bar{n}_t n_u\delta_{rt}V_{uq[ps]}\frac{1}{\epsilon_u+\epsilon_q-\epsilon_p-\epsilon_s}\frac{1}{\omega_f-\epsilon_s+\epsilon_u+i0^+}\\
&\cdot\frac{1}{\omega-\epsilon_s-\epsilon_t+\epsilon_u+i0^+}\frac{1}{\omega_i-\epsilon_t+\epsilon_u+i0^+}\\
3e &= n_p\bar{n}_q\bar{n}_r n_s\bar{n}_t\bar{n}_u\delta_{rt}V_{uq[ps]}\frac{1}{\omega_f+\epsilon_p-\epsilon_q+i0^+}\frac{1}{\omega+\epsilon_p-\epsilon_q-\epsilon_r+i0^+}\\
&\cdot\frac{1}{\omega_i+\epsilon_p-\epsilon_q-\epsilon_r+\epsilon_s+i0^+}\frac{1}{-\epsilon_u-\epsilon_q+\epsilon_p+\epsilon_s}\\
4a &= n_p\bar{n}_q\bar{n}_r n_s\bar{n}_t n_u\delta_{su}V_{rq[pt]}\frac{1}{\omega_f+\epsilon_p-\epsilon_q+i0^+}\frac{1}{\omega+\epsilon_p-\epsilon_q-\epsilon_r+i0^+}\\
&\cdot\frac{1}{\omega-\epsilon_t+i0^+}\frac{1}{\omega_i-\epsilon_t+\epsilon_u+i0^+}\\
4b &= n_p\bar{n}_q\bar{n}_r n_s\bar{n}_t n_u\delta_{su}V_{rq[pt]}\frac{1}{\omega_f+\epsilon_p-\epsilon_q+i0^+}\frac{1}{\omega+\epsilon_p-\epsilon_q-\epsilon_r+i0^+}\\
&\cdot\frac{1}{\omega_i+\epsilon_p-\epsilon_q-\epsilon_r+\epsilon_s+i0^+}\frac{1}{\omega_i-\epsilon_t+\epsilon_u+i0^+}\\
4c &= -n_p\bar{n}_q n_r n_s\bar{n}_t n_u\delta_{su}V_{rq[pt]}\frac{1}{\omega_f+\epsilon_p-\epsilon_q+i0^+}\frac{1}{\omega_f+\epsilon_r-\epsilon_t+i0^+}\\
&\cdot\frac{1}{\omega-\epsilon_t+i0^+}\frac{1}{\omega_i-\epsilon_t+\epsilon_u+i0^+}\\
4d &= -\bar{n}_p n_q n_r n_s\bar{n}_t n_u\delta_{su}V_{rq[pt]}\frac{1}{\epsilon_r+\epsilon_q-\epsilon_p-\epsilon_t}\frac{1}{\omega_f+\epsilon_r-\epsilon_t+i0^+}
\end{aligned}
$$

$$\cdot\frac{1}{\omega-\epsilon_t+i0^+}\frac{1}{\omega_i-\epsilon_t+\epsilon_u+i0^+}$$

$$4e = -n_p\bar{n}_q\bar{n}_r n_s n_t n_u\delta_{su}V_{rq[pt]}\frac{1}{\omega_f+\epsilon_p-\epsilon_q+i0^+}\frac{1}{\omega+\epsilon_p-\epsilon_q-\epsilon_r+i0^+}$$
$$\cdot\frac{1}{\omega_i+\epsilon_p-\epsilon_q-\epsilon_r+\epsilon_u+i0^+}\frac{1}{-\epsilon_r-\epsilon_q+\epsilon_p+\epsilon_t}$$

$$5a = n_p\bar{n}_q\bar{n}_r\bar{n}_s\bar{n}_t n_u\delta_{qs}V_{ur[pt]}\frac{1}{\omega_f+\epsilon_p-\epsilon_q+i0^+}\frac{1}{\omega+\epsilon_p-\epsilon_q-\epsilon_r+i0^+}$$
$$\cdot\frac{1}{\omega-\epsilon_s-\epsilon_t+\epsilon_u+i0^+}\frac{1}{\omega_i-\epsilon_t+\epsilon_u+i0^+}$$

$$5b = n_p\bar{n}_q\bar{n}_r\bar{n}_s\bar{n}_t n_u\delta_{qs}V_{ur[pt]}\frac{1}{\omega_f+\epsilon_p-\epsilon_q+i0^+}\frac{1}{\omega+\epsilon_p-\epsilon_q-\epsilon_r+i0^+}$$
$$\cdot\frac{1}{\omega_i+\epsilon_p-\epsilon_r+i0^+}\frac{1}{\omega_i-\epsilon_t+\epsilon_u+i0^+}$$

$$5c = -n_p\bar{n}_q n_r\bar{n}_s\bar{n}_t n_u\delta_{qs}V_{ur[pt]}\frac{1}{\omega_f+\epsilon_p-\epsilon_q+i0^+}\frac{1}{\omega_f+\epsilon_r-\epsilon_s-\epsilon_t+\epsilon_u+i0^+}$$
$$\cdot\frac{1}{\omega-\epsilon_s-\epsilon_t+\epsilon_u+i0^+}\frac{1}{\omega_i-\epsilon_t+\epsilon_u+i0^+}$$

$$5d = \bar{n}_p\bar{n}_q n_r\bar{n}_s\bar{n}_t n_u\delta_{qs}V_{ur[pt]}\frac{1}{\epsilon_u+\epsilon_r-\epsilon_p-\epsilon_t}\frac{1}{\omega_f-\epsilon_q+\epsilon_r-\epsilon_t+\epsilon_u+i0^+}$$
$$\cdot\frac{1}{\omega-\epsilon_s-\epsilon_t+\epsilon_u+i0^+}\frac{1}{\omega_i-\epsilon_t+\epsilon_u+i0^+}$$

$$5e = n_p\bar{n}_q\bar{n}_r\bar{n}_s n_t\bar{n}_u\delta_{qs}V_{ur[pt]}\frac{1}{\omega_f+\epsilon_p-\epsilon_q+i0^+}\frac{1}{\omega+\epsilon_p-\epsilon_q-\epsilon_r+i0^+}$$
$$\cdot\frac{1}{\omega_i+\epsilon_p-\epsilon_r+i0^+}\frac{1}{-\epsilon_u-\epsilon_r+\epsilon_p+\epsilon_t}$$

$$6a = n_p\bar{n}_q n_r\bar{n}_s\bar{n}_t n_u\delta_{pr}V_{uq[st]}\frac{1}{\omega_f+\epsilon_p-\epsilon_q+i0^+}\frac{1}{\omega-\epsilon_q+i0^+}$$
$$\cdot\frac{1}{\omega-\epsilon_s-\epsilon_t+\epsilon_u+i0^+}\frac{1}{\omega_i-\epsilon_t+\epsilon_u+i0^+}$$

$$6b = -n_p\bar{n}_q n_r n_s\bar{n}_t n_u\delta_{pr}V_{uq[st]}\frac{1}{\omega_f+\epsilon_p-\epsilon_q+i0^+}\frac{1}{\omega-\epsilon_q+i0^+}$$
$$\cdot\frac{1}{\omega_i-\epsilon_q+\epsilon_s+i0^+}\frac{1}{\omega_i-\epsilon_t+\epsilon_u+i0^+}$$

$$6c = n_p\bar{n}_q n_r\bar{n}_s\bar{n}_t n_u\delta_{pr}V_{uq[st]}\frac{1}{\omega_f+\epsilon_p-\epsilon_q+i0^+}\frac{1}{\omega_f+\epsilon_r-\epsilon_s-\epsilon_t+\epsilon_u+i0^+}$$
$$\cdot\frac{1}{\omega-\epsilon_s-\epsilon_t+\epsilon_u+i0^+}\frac{1}{\omega_i-\epsilon_t+\epsilon_u+i0^+}$$

$$6d = -n_p n_q n_r\bar{n}_s\bar{n}_t n_u\delta_{pr}V_{uq[st]}\frac{1}{\epsilon_u+\epsilon_q-\epsilon_s-\epsilon_t}\frac{1}{\omega_f+\epsilon_p-\epsilon_s-\epsilon_t+\epsilon_u+i0^+}$$
$$\cdot\frac{1}{\omega-\epsilon_s-\epsilon_t+\epsilon_u+i0^+}\frac{1}{\omega_i-\epsilon_t+\epsilon_u+i0^+}$$

$$6e \;=\; -n_p\bar{n}_q n_r n_s n_t \bar{n}_u \delta_{pr} V_{uq[st]} \frac{1}{\omega_f + \epsilon_p - \epsilon_q + i0^+} \frac{1}{\omega - \epsilon_q + i0^+} \cdot \frac{1}{\omega_i - \epsilon_q + \epsilon_s + i0^+} \frac{1}{-\epsilon_u - \epsilon_q + \epsilon_s + \epsilon_t}$$

2. Four-times Green's function for a closed-shell anion

The diagrams of Fig.9 are simply numbered from 1 to 5. Their contributions are:

$$1 \;=\; -n_p\bar{n}_q\bar{n}_r n_s V_{qs[rp]} \frac{1}{\omega_f + \epsilon_p + i0^+} \frac{1}{\omega + \epsilon_p - \epsilon_q + i0^+} \cdot \frac{1}{\omega - \epsilon_r + \epsilon_s + i0^+} \frac{1}{\omega_i + \epsilon_s + i0^+}$$

$$2 \;=\; n_p\bar{n}_q n_r n_s V_{qs[rp]} \frac{1}{\omega_f + \epsilon_p + i0^+} \frac{1}{\omega + \epsilon_p - \epsilon_q + i0^+} \cdot \frac{1}{\omega_i + \epsilon_p - \epsilon_q + \epsilon_r + i0^+} \frac{1}{\omega_i + \epsilon_s + i0^+}$$

$$3 \;=\; n_p n_q\bar{n}_r n_s V_{qs[rp]} \frac{1}{\omega_f + \epsilon_p + i0^+} \frac{1}{\omega_f + \epsilon_q - \epsilon_r + \epsilon_s + i0^+} \cdot \frac{1}{\omega - \epsilon_r + \epsilon_s + i0^+} \frac{1}{\omega_i + \epsilon_s + i0^+}$$

$$4 \;=\; -\bar{n}_p n_q\bar{n}_r n_s V_{qs[rp]} \frac{1}{\epsilon_q + \epsilon_s - \epsilon_r - \epsilon_p} \frac{1}{\omega_f + \epsilon_q - \epsilon_r + \epsilon_s + i0^+} \cdot \frac{1}{\omega - \epsilon_r + \epsilon_s + i0^+} \frac{1}{\omega_i + \epsilon_s + i0^+}$$

$$5 \;=\; -n_p\bar{n}_q n_r\bar{n}_s V_{qs[rp]} \frac{1}{\omega_f + \epsilon_p + i0^+} \frac{1}{\omega + \epsilon_p - \epsilon_q + i0^+} \cdot \frac{1}{\omega_i + \epsilon_p - \epsilon_q + \epsilon_r + i0^+} \frac{1}{-\epsilon_q - \epsilon_s + \epsilon_r + \epsilon_p}$$

3. Three-times Green's function for a closed-shell anion

The diagrams of Fig.19 are simply numbered from 1 to 4. Their contributions are:

$$1 \;=\; n_p n_q\bar{n}_r n_s V_{rs[pq]} \frac{1}{\omega + \epsilon_p + i0^+} \frac{1}{\omega' + \epsilon_p + \epsilon_q - \epsilon_r + i0^+} \frac{1}{\omega' + \epsilon_s + i0^+}$$

$$2 \;=\; n_p\bar{n}_q n_r n_s V_{qs[rp]} \frac{1}{\omega + \epsilon_p + i0^+} \frac{1}{\omega - \epsilon_q + \epsilon_r + \epsilon_s + i0^+} \frac{1}{\omega' + \epsilon_s + i0^+}$$

$$3 \;=\; -\bar{n}_p\bar{n}_q n_r n_s V_{qs[rp]} \frac{1}{\epsilon_r + \epsilon_s - \epsilon_p - \epsilon_q} \frac{1}{\omega - \epsilon_q + \epsilon_r + \epsilon_s + i0^+} \frac{1}{\omega' + \epsilon_s + i0^+}$$

$$4 \;=\; -n_p n_q\bar{n}_r\bar{n}_s V_{qs[rp]} \frac{1}{\omega + \epsilon_p + i0^+} \frac{1}{\omega' + \epsilon_p + \epsilon_q - \epsilon_r + i0^+} \frac{1}{-\epsilon_r - \epsilon_s + \epsilon_p + \epsilon_q}$$

[1] J. Schirmer, L. S. Cederbaum, and O. Walter, Phys. Rev. A 28, 1237 (1983).

[2] M. Deleuze, Int. J. Quantum Chem. 93, 191 (2003).

[3] M. Ohno, V. G. Zakrzewski, J. V. Ortiz, and W. von Niessen, J. Chem. Phys. 106, 3258 (1997).

[4] J. V. Ortiz, Int. J. Quantum Chem. 95, 593 (2003).

[5] L. S. Cederbaum, in *Enzyclopedia of Quantum Chemistry*, edited by P. v. R. Schleyer et al. (Wiley, Chichester, 1998).

[6] J. S. Bell and E. J. Squires, Phys. Rev. Lett. 3, 96 (1959).

[7] H. Feshbach, Ann. Phys. 19, 287 (1962).

[8] B. Schneider, H. S. Taylor, and R. Yaris, Phys. Rev. A 1,855 (1970).

[9] Gy. Csanak, H. S. Taylor, and R. Yaris, Phys. Rev. A 3, 1322 (1971).

[10] A. Klonover and U. Kaldor, Chem. Phys. Lett. 51, 321 (1977); J. Phys. B 11, 1623 (1978).

[11] M. Berman, O. Walter, and L. S. Cederbaum, Phys. Rev. Lett. 50, 1979 (1983).

[12] H.-D. Meyer, Phys. Rev. A 40, 5605 (1989).

[13] F. Capuzzi and C. Mahaux, Ann. Phys. NY 239,57 (1995).

[14] F. Michel and G. Reidemeister, Phys. Rev. C 53, 3032 (1996).

[15] G. Csanak, D. C. Cartwright, and F. J. da Paixao, Phys. Rev. A 48, 2811 (1993).

[16] D. C. Cartwright and G. Csanak, Phys. Rev. A 51, 454 (1995).

[17] L. V. Keldysh, Zh. Eksp. Teor. Fis. 47, 1515 (1964) [Sov. Phys. JETP 20, 1018 (1965)].

[18] L. S. Cederbaum, Few-Body Syst. 21, 211 (1996).

[19] P. Winkler and L. S. Cederbaum, Phys. Rev. A 61, 052701 (2000).

[20] L. S. Cederbaum, Phys. Rev. Lett. 85, 3072 (2000).

[21] L. S. Cederbaum, Ann. Phys. 291, 169 (2001).

[22] P. Winkler, S.-T. Dai, Int. J. Quantum Chem. 85, 257 (2001).

[23] J. Brand, L. S. Cederbaum, and H.-D. Meyer, Phys. Rev. A 60, 2983 (1999).

[24] J. T. Golab and D. L. Yeager, J. Chem. Phys. 87, 2925 (1987); D. L. Yeager, J. A. Nichols, and J. T. Golab, J. Chem. Phys. 98, 8790 (1993); A. McKellar and D. L. Yeager, Chem. Phys. 238, 1 (1998).

[25] O. E. Alon und L. S. Cederbaum, J. Phys. A 35, L303 (2002).

[26] S. Ethofer, P. Schuck, Z. Phys. 228, 264 (1969).

[27] J. Schirmer, Phys. Rev. A 26, 2395 (1982).

[28] A. L. Fetter and J. D. Walecka, *Quantum Theory of Many-Particle Systems*, 1st ed. (McGraw-Hill, New York, 1971).

[29] A. B. Migdal, *Theory of Finite Fermi Systems* (Wiley-Interscience, New York, 1967).

[30] J. Schirmer, A. B. Trofimov, and G. Stelter, J. Chem. Phys. 109, 4734 (1998); A. B. Trofimov, G. Stelter, and J. Schirmer, J. Chem. Phys. 111, 9982 (1999).

[31] J. Schirmer, A. B. Trofimov, J. Chem. Phys. 120, 11449 (2004).